AD-A283 274

PL-TR-94-2014

AN INVESTIGATION OF SMALL-SCALE VARIATIONS IN CLOUD CLIMATOLOGY INDUCED BY TOPOGRAPHY AND MONTHLY MEAN WINDS

James H. Willand, Albert R. Boehm, and Gary Gray

Hughes STX Corporation
109 Massachusetts Avenue
Lexington, MA 02173

21 January, 1994

Scientific Report No. 3

APPROVED FOR PUBLIC RELEASE; DISTRIBUTION UNLIMITED.

PHILLIPS LABORATORY
Directorate of Geophysics
AIR FORCE MATERIEL COMMAND
HANSCOM AIR FORCE BASE, MA 01731-3010

"This technical report has been reviewed and is approved for publication"

Donald D. Grantham

DONALD D. GRANTHAM
Contract Manager
Chief, Atmospheric Structure Branch

Robert A. McClatchey

ROBERT A. McCLATCHEY
Director, Atmospheric Sciences Division

This report has been reviewed by the ESC Public Affairs Office (PA) and is releasable to the National Technical Information Service (NTIS).

Qualified requestors may obtain additional copies from the Defense Technical Information Center. All others should apply to the National Technical Information Service.

If your address has changed, or if you wish to be removed from the mailing list, or if the addressee is no longer employed by your organization, please notify PL/TSI, Hanscom AFB, MA 01731-3010. This will assist us in maintaining a current mailing list.

Do not return copies of this report unless contractual obligations or notices on a specific document requires that it be returned.

REPORT DOCUMENTATION PAGE

Form Approved
OMB No. 0704-0188

1. AGENCY USE ONLY *(Leave blank)*

2. REPORT DATE
21 January 1994

3. REPORT TYPE AND DATES COVERED
Scientific Report # 3

4. TITLE AND SUBTITLE
AN INVESTIGATION OF SMALL-SCALE VARIATIONS IN CLOUD CLIMATOLOGY INDUCED BY TOPOGRAPHY AND MONTHLY MEAN WINDS

5. FUNDING NUMBERS
F19628-93-C-0051
PE62101F
PR6670
TA GS
WU AC

6. AUTHOR(S)
James H. Willand, Albert R. Boehm, and Gary Gray

7. PERFORMING ORGANIZATION NAME(S) AND ADDRESS(ES)
Hughes STX Corporation
109 Massachusetts Avenue
Lexington, MA 02173

8. PERFORMING ORGANIZATION REPORT NUMBER
Hughes STX Scientific Report #3

9. SPONSORING/MONITORING AGENCY NAME(S) AND ADDRESS(ES)
Phillips Laboratory
29 Randolph Road
Hanscom AFB, MA 01731-3010

Contract Technical Manager: Donald D. Grantham/GPAA

10. SPONSORING/MONITORING AGENCY REPORT NUMBER
PL-TR-94-2014

11. SUPPLEMENTARY NOTES

12a. DISTRIBUTION/AVAILABILITY STATEMENT
Approved for public release: distribution unlimited.

12b. DISTRIBUTION CODE

13. ABSTRACT *(Maximum 200 words)*

This report is an assessment of the use of vector mean wind components and terrain heights to indicate the occurrence of terrain-induced small-scale cloud amount conditions.

14. SUBJECT TERMS
Clouds, climatology, coverage, terrain, wind vectors

15. NUMBER OF PAGES
48

16. PRICE CODE

17. SECURITY CLASSIFICATION OF REPORT	18. SECURITY CLASSIFICATION OF THIS PAGE	19. SECURITY CLASSIFICATION OF ABSTRACT	20. LIMITATION OF ABSTRACT
Unclassified	Unclassified	Unclassified	Unlimited

TABLE OF CONTENTS

Section **Page**

1. Introduction

This report is an assessment of the use of vector mean wind components and terrain heights to indicate the occurrence of terrain-induced small scale cloud amount conditions. It is anticipated that the results of this study will lead to the implementation of indicators (topology, land or sea, upslopes, etc.) that will improve sky cover quantification within compact fast-retrieval computerized systems of global cloud climatologies like those by Boehm and Willand, 1993, called C Cloud S.

Given any location on earth at any given time of year and time of day, program C Cloud S uses indicators in the form of coefficients to determine various cloud statistics. Presently coefficients stored within the C Cloud S system are used to quantify five parameters essential for defining the cloud statistics. The five parameters are 1) mean sky covers; 2) sky dome mean correlations; 3) large area size mean correlations; 4) sample size of original sky cover observations; and 5) interannual standard deviation of sky cover. In general these synthesized or indicated parameters are computed by C Cloud S using

$$\begin{aligned} P_r &= F(\theta, \lambda, D, h) \\ &\text{where} \\ \theta &= \text{Latitude} \\ \lambda &= \text{Longitude} \\ D &= \text{Time of year} \\ h &= \text{Time of day} \\ P_r &= \text{Indicated parameter.} \end{aligned} \qquad \ldots\ldots \quad (1)$$

Sky cover indicators for large areas of the earth's surface are proving accurate, but indicators are required for smaller areas of the world where terrain and land ocean boundary effects influence the sky cover conditions. In order to provide for more accurate indication of sky cover probabilities over these areas, it is proposed that two more parameters be included within the equation such that

$$P_r = F(\sigma, \lambda, D, h, T_z, \overline{u}) \quad \text{where} \quad T_z = \text{Terrain height}, \quad \overline{u} = \text{vector mean wind direction component.} \qquad \ldots \quad (2)$$

Here it is assumed that terrain height and the vector mean wind direction component for a given location are the two additional parameters necessary for defining the probable small scale sky cover conditions. This report is an assessment of that assumption.

2. Databases

The databases utilized in this investigation are described in this section.

2.1 Clouds

Two climatological cloud databases are utilized in this study. They are 1) the automated Climatology of Cloud Statistics, "C Cloud S" and 2) a subset of the USAF Real Time Nephanalysis, "RTNEPH" called the Total Histogram Cloud Data Tapes, "THCT". The two databases are discussed below.

2.1.1 C Cloud S

C Cloud S isn't a cloud database per se. It is a computerized system designed for rapid access of global cloud statistics which are based on actual cloud cover climatologies. Willand (1992) discussed the three sources of cloud cover climatologies used in developing the C Cloud S system. The first, called Burger data (Burger, 1985), consisted of mean sky covers, sky cover density distributions, and computed scale distances. The statistics were based on surface observations of sky cover collected from more than 2300 stations around the world. The data period of record was 29 years from 1945 to 1974. The second database used was the "Climatological Data for Clouds Over the Globe from Surface Observations" (Hahn, 1987). The portion of this database that was used in the development of C Cloud S was the seasonal averages and variances of sky covers archived into 5 X 5 degree grid boxes and mapped over the globe for 8 times of day, i.e. 00,03,06 ... 21 GMT. The period of

record for sky cover observations from land observers was 11 years and for those over the oceans was 54 years. The third cloud database used was the NIMBUS-7 Cmatrix cloud cover data (Hwang,et al, 1988) archived over a 6 year period of record from April 1979 thru March 1985. The portion of this database used was the mean and computed variances of cloud cover amounts that were derived from the NIMBUS 7 satellite observed radiances and mapped into 2070 Earth Radiation Budget target areas each representing a 500 X 500 km equal area. These satellite cloud statistics were archived twice a day at noon and midnight.

The three cloud databases were input to a weighted spectral analysis program (WESPAN) which used a weighted associated Legendre function in latitude and a Fourier function in longitude to compress the large amounts of data into the form of coefficients. The coefficients derived from each of the three data ensembles were then blended together to form a single set of coefficients capable of indicating several types of cloud statistics over any given point in the world for any given time.

Figure 1. shows a C Cloud S world-wide pattern map of indicated percent mean sky covers for January at 00 mean apparent sun time, MAST. Note that overall, the indications of sky covers are very good. That is, very low mean sky cover percentages (10 - 20%) can be found over the Middle East, higher percentages (70 - 90%) can be seen over the Amazon in South America, and again lower sky cover amounts (20 - 30%) are indicated over the Gibson and Great Victoria deserts of Australia. What is lacking is the indication of the smaller scaled terrain induced cloud cover effects that can occur over land-sea boundaries and valleys or mountainous regions of the globe. (The smoothing over of small scale sky cover effects due to terrain by C Cloud S will become more apparent in the higher resolution depictions of indicated cloud covers shown in later sections.)

2.1.2 RTNEPH (TCHT)

The Real Time Nephanalysis (RTNEPH) data is an ensemble of cloud amount and cloud layer statistics collected daily on a

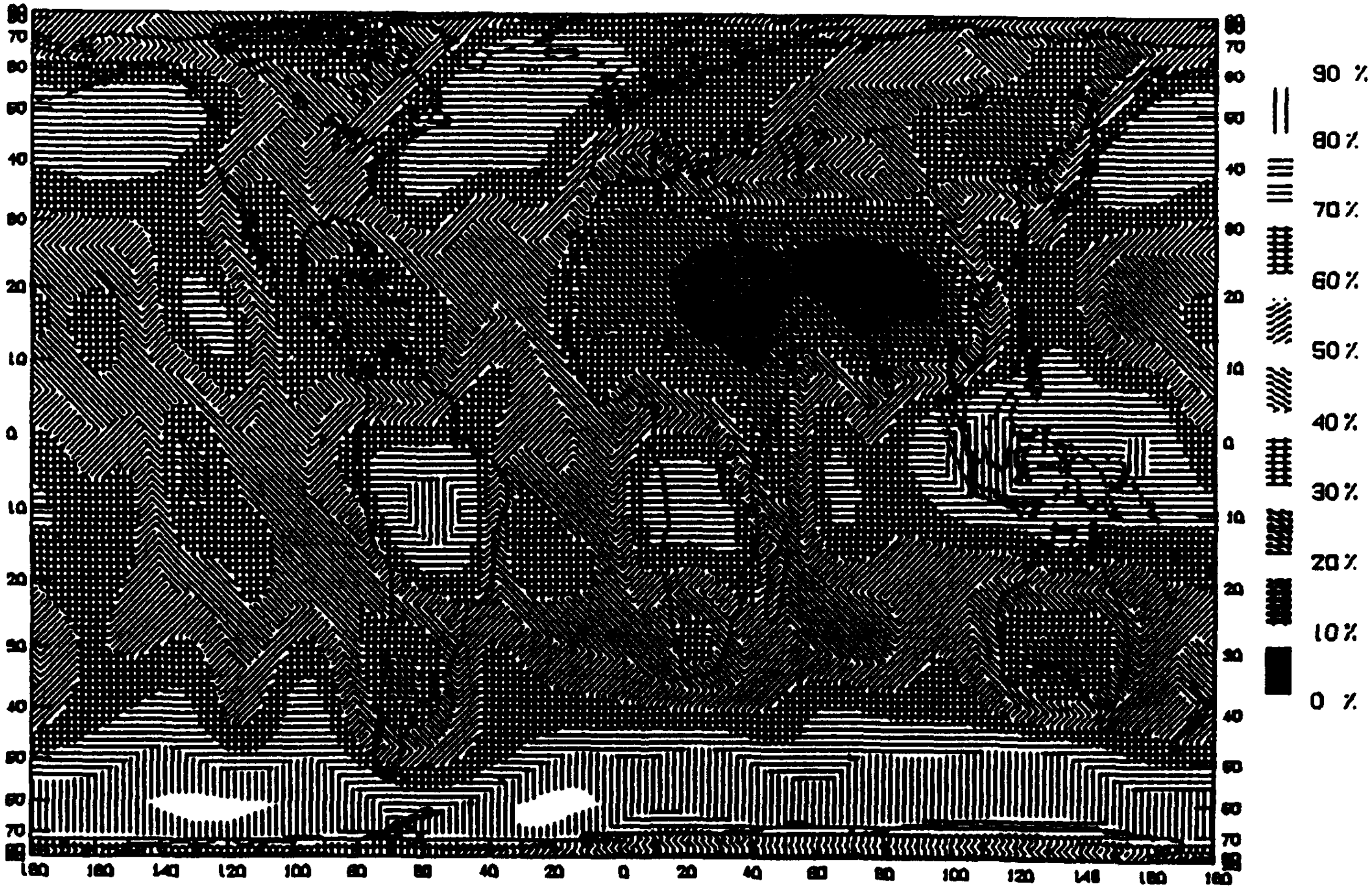

Figure 1. Pattern Map of Indicated Mean Sky Cover for January at 00 MAST. Indicators were accomplished by a main frame computer version of C Cloud S.

real-time basis by the USAF. The data are archived 8 times of day, i.e. 00,03,06 ...21 GMT. Most of the cloud statistics are derived from observed satellite visible and infrared radiances but surface observed sky cover conditions are also inserted into the data base. There are several known problems with this database. Some of the problems are as follows:

- Underestimation of low cloud by the satellite IR sensors can occur where cloud top temperatures exceed or equal background temperatures.
- Cold snow/ice covered areas can be interpreted as cloud.
- Clouds smaller than satellite sensor resolution can be underinterpreted.
- Possible overinterpretation of clouds can occur over high plateaus.
- Satellite viewing angle correction is not taken into account.
- Insertion of ground observed sky cover conditions can seriously disrupt the homogeneous cloud cover conditions and distributions that otherwise would have been derived from the satellite radiances when developing cloud climatologies. See Boehm, et al (1992).

See Dalcher (1992, Appendix B) for a good summary of problems associated with the RTNEPH data.

The RTNEPH data are mapped into polar projections for the Northern and Southern hemispheres, Figure 2., (Hoke, 1981). Each map is divided into 64 large boxes. Each large box is further divided into 64 X 64 smaller boxes, each having an approximate resolution of 25 nautical miles or 46.3 kilometers. A subset of these data were derived by the USAFETAC operations group. The subset is called the "Total Cloud Histogram Tapes", (TCHT). The tapes were acquired by GPAA and are the primary source of data used in this study. The data were archived in the same mapping configuration discussed above, but instead of using the standard RTNEPH format, data were categorized and mapped in the form of a histogram for each small box over a 5 year period of record from

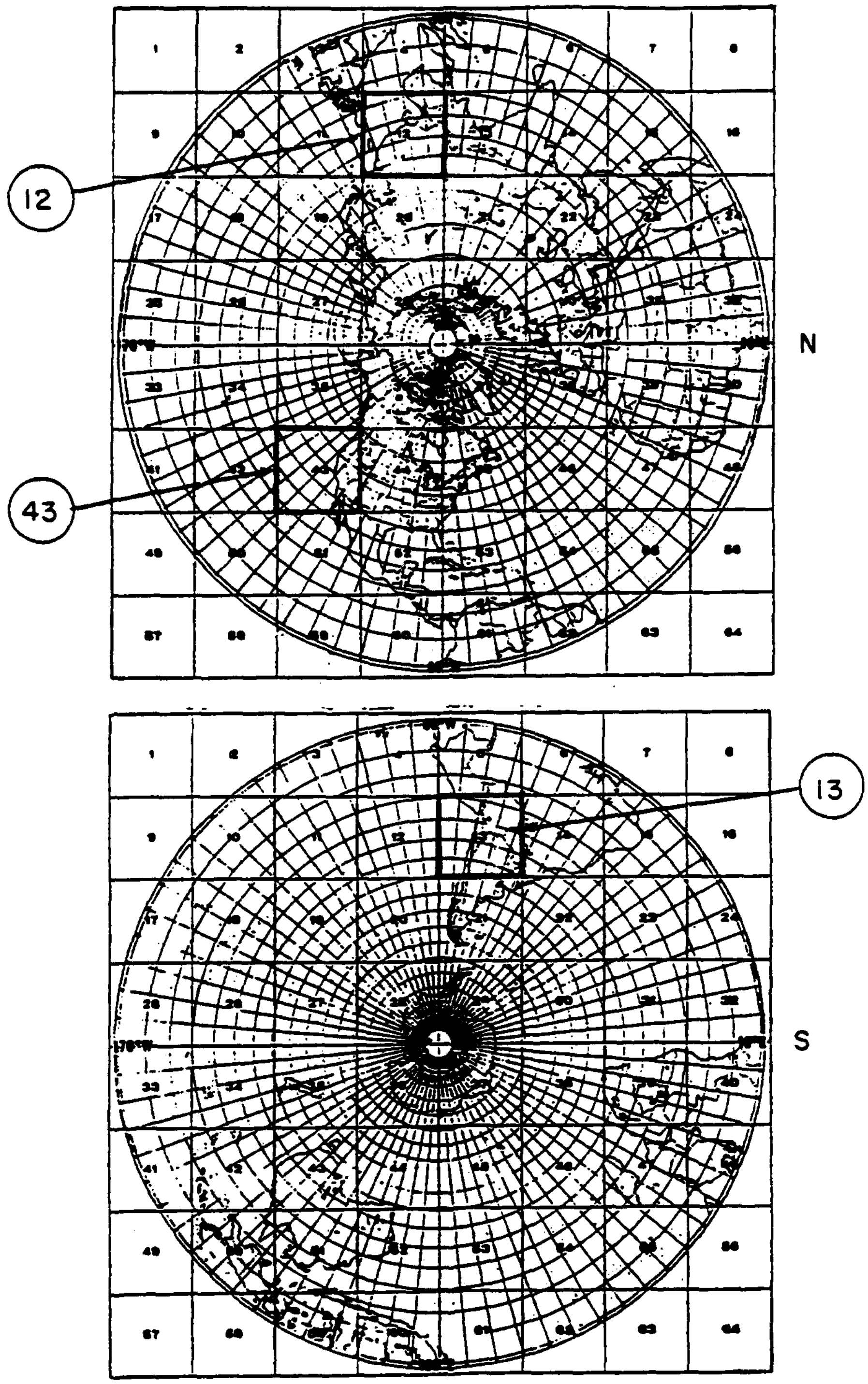

Figure 2. The Northern (Top) and Southern (Bottom) Polar Stereographic Map Projections used for Archiving the RTNEPH Data. The 64 Mesh Large Boxes Within Each Map are Indicated. The RTNEPH Grid Boxes 12 and 43 in the Northern Hemisphere and Box Number 13 in the Southern Hemisphere are the Areas of Study.

1985 through 1989. It is therefore a climatology of RTNEPH cover in histogram form. Each histogram has 22 bins. Twenty one bins contain the frequency of occurrence of a categorized cloud amount such as that shown in Table 1. The 22nd bin contains the frequency of missing/bad cloud amount data. These data were assembled as two sets per month, with statistics for 8 times of day. The first set of data was accumulated over days 1 thru 15. The second set was accumulated for days 16 through the end of the month. Means and standard deviations of cloud covers for each box in the TCHT database were not archived. The following methodologies were used to calculate the mean and standard deviations of cloud cover.

The computation of the mean cloud cover ($\bar{a}$) given a TCHT density distribution of cloud amount for a given RTNEPH small box is computed in (3)

$$\bar{a} = \sum_{i=1}^{21} p_i \, a_i \quad \ldots\ldots\ldots\ldots \quad (3)$$

where:

p_i = probability of cloud amount in category i. p_i is computed through use of (4)

where:

$$p_i = \frac{f_i}{\sum_{i=1}^{21} f_i} \quad \ldots\ldots\ldots\ldots \quad (4)$$

where:

f = frequency of cloud amount in category i.

a_i = fractional cloud amount at middle of category i (Table 1.).

$\bar{a}$ = mean cloud amount

i = index of Table 1.

The standard deviations s of the mean cloud amount is computed by calculating the value of $\bar{a}^2$,

$$\overline{a^2} = \sum_{i=1}^{21} p_i a_i^2 \quad , \qquad (5)$$

and determining standard deviation, s, from (6)

$$s = \sqrt{\overline{a^2} - (\overline{a})^2} \quad . \qquad (6)$$

Table 1. Cloud Amount Categories for TCHT Data.

Index	Category	Mid Pnt.
1	.0	.0
2	.01 - .05	.025
3	.06 - .10	.075
4	.11 - .15	.125
5	.16 - .20	.175
6	.21 - .25	.225
7	.26 - .30	.275
8	.31 - .35	.325
9	.36 - .40	.375
10	.41 - .45	.425
11	.46 - .50	.475
12	.51 - .55	.525
13	.56 - .60	.575
14	.61 - .65	.625
15	.66 - .70	.675
16	.71 - .75	.725
17	.76 - .80	.775
18	.81 - .85	.825
19	.86 - .90	.875
20	.91 - .95	.925
21	.96 -1.00	1.000

2.2 Terrain

The hemispheric eighth mesh terrain elevation data upgraded by Schaaf, et al (1990) was chosen to represent land-sea boundaries and terrain heights in this study. The elevations are archived in the same hemispheric eighth mesh (approximate 25 nautical mile resolution) grid system as that of the RTNEPH. Therefore, there is a mean elevation (meters) archived for each RTNEPH small box.

2.3 Wind

To assist in the computation of upslope probabilities a world wide database of mean monthly wind components prepared by the European Center for Median-Range Weather Forecasts (ECMWF) was acquired from the USAFETAC. The database acquired was for the 500 millibar level only. It is assumed that the mean wind components at this level represent typical wind conditions over hilly terrain areas. The archived wind components within this database are:

$\bar{u}$ = tenths of meters/sec

S_u= Standard deviation of $\bar{u}$

$\bar{v}$ = tenths of meters/sec

S_v= Standard deviation of $\bar{v}$.

These mean wind components were archived monthly over a ten year period of record for every 2.5 degrees of latitude and longitude.

3. Experiments

Two experiments were conducted to determine the usefulness of terrain height information and/or mean wind components to indicate probable occurrences of terrain induced cloud amounts. The first experiment looked at land-sea boundary areas to see if cloud amount distributions derived over land differed significantly from those derived over the nearby ocean. The second experiment correlated terrain upslope probabilities with actual satellite cloud amount climatology minus indicated cloud cover climatologies.

The three regions of RTNEPH-TCHT data outlined in Figure 2 were selected for investigation. As shown in the figure, RTNEPH

box number 12 encompasses Eastern Asia, the South China Sea, and Taiwan. Box 43 includes the West Coast of the USA and a large portion of the Eastern Pacific Ocean. Finally, box number 13 in the southern hemisphere covers the West Coast of central South America along the Andes Mountains in Chile and a portion of the Eastern Pacific Ocean. These areas were selected because of their hilly terrain, proximity to land-ocean boundaries, known land-ocean cloud effects, and apparently clean RTNEPH data.

3.1 Land-Sea

It is known that several of the worlds land-sea boundary areas have profound effects on cloud cover conditions. The persistent low lying marine stratus off the California coast is a well known example. Cloud conditions over the eastern Pacific ocean bordering the central west coast of South America are influenced by ocean upwelling within that area.

The Land-Sea experiment was a simple test to see if differences of percent of RTNEPH amounts minus indicated C Cloud S cloud amounts over land versus those over the adjacent ocean area are of significance. To accomplish this comparison, a program called rtnmean.f was written to first read in the entire TCHT data for a given RTNEPH grid box (64 X 64 small boxes). The mean and the standard deviation of the cloud amount were computed for each box using the methodologies described in 2.1.2. The terrain heights for the corresponding box were also read in from the hemispheric eighth mesh terrain elevation database. Coefficients for indicating mean cloud amount over each small box within a given area were also input. This entailed the input of C Cloud S coefficients for indicating mean sky cover and mean correlation for a given month at the mean apparent sun time closest to the center of the given RTNEPH box desired. Thus, coefficients for January at 0900 MAST were used with data for box 12, 1500 MAST for box 43, and 1800 MAST for box 13 in the Southern Hemisphere. Indicated mean sky covers derived from these coefficients reflect sky conditions as seen over a sky dome (up-looking). Since the RTNEPH cloud data are mostly from

satellites, these indicated sky covers were adjusted for down-looking cloud cover conditions using (8) below. (Boehm, et al, 1991).

$$ccld = .25p + .75(s^2 + p^2) \quad \cdots\cdots\cdots \quad (7)$$

where

p = indicated probability of sky cover amount

s = standard deviation of p computed from C Cloud S indicated mean correlation.

ccld = cloud cover looking down.

Figures 3, 4, and 5 show the results of the land-sea comparisons for the three selected RTNEPH box areas (12,43, and 13 respectively). In each graph the horizontal axis signifies the percent difference of mean RTNEPH amount minus the C Cloud S indicated cloud amount over each small box within most of the area presented in the upper right corner of each figure. The vertical axis signifies the unnormalized counts of such events. These events are portrayed for both land and ocean conditions. Discrimination of small boxes over land from those over ocean was made using the 8th mesh terrain elevation data. Counts shown in Figure 3 were made for all small boxes eastward of 105 deg's east. In Figure 4 counts were tallied eastward of 120 deg's, and in Figure 5 westward of 65 deg's.

The Figure 3 case over Eastern Asia and the China sea shows that about half of the RTNEPH amounts are below indicated cloud amounts for observations over the ocean. Most RTNEPH cloud amounts over land were greater than indicated amounts, some by as much as 30 %.

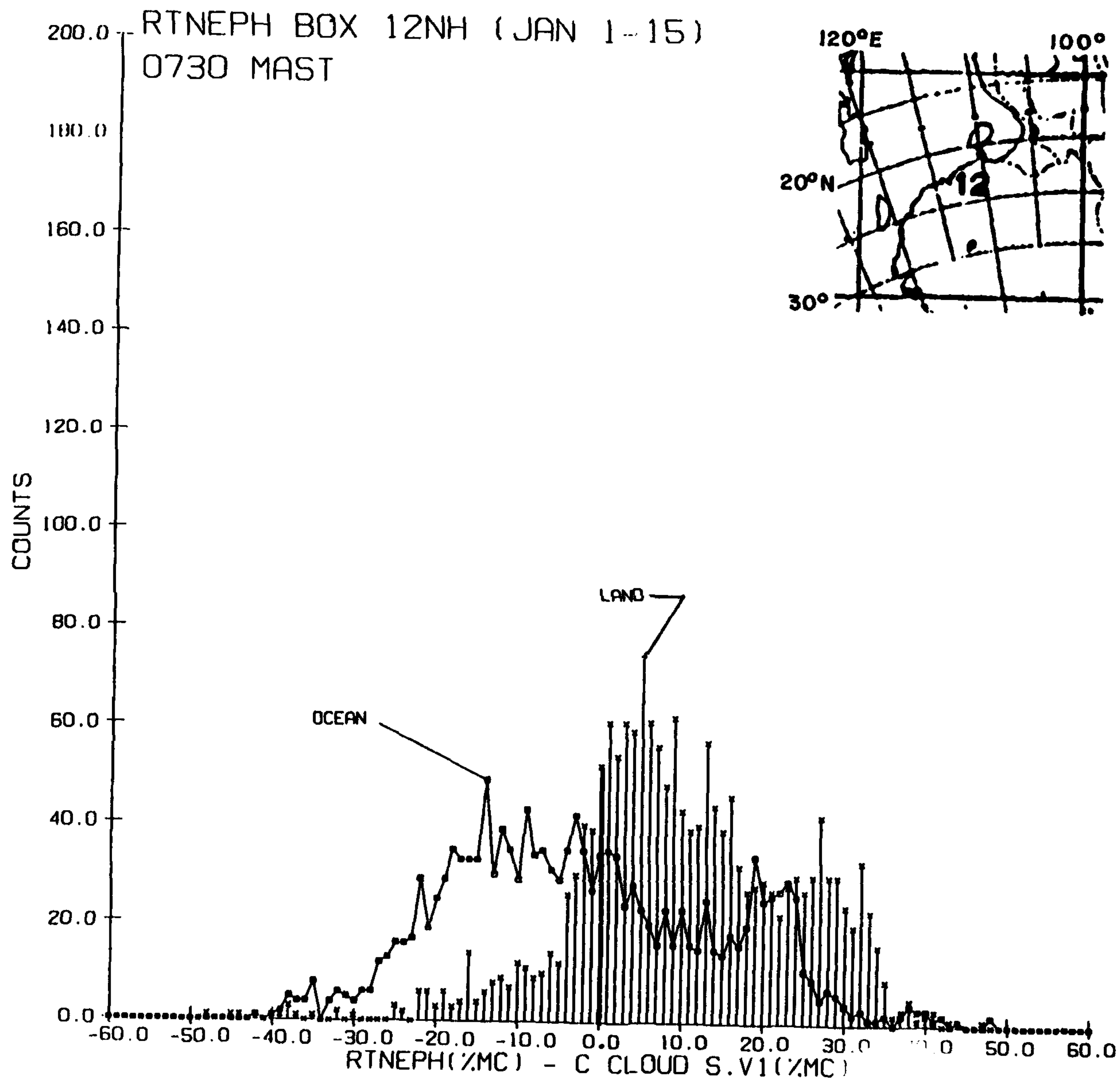

Figure 3. Counts of Percent Mean Cloud Cover (%MC) for Jan. 1-15 RTNEPH TCHT Data Minus C Cloud S Indicated Percent Mean Cloud Cover Over Land Versus Those Over the Adjacent Ocean Area for Region 12 East of 105 Degs East.

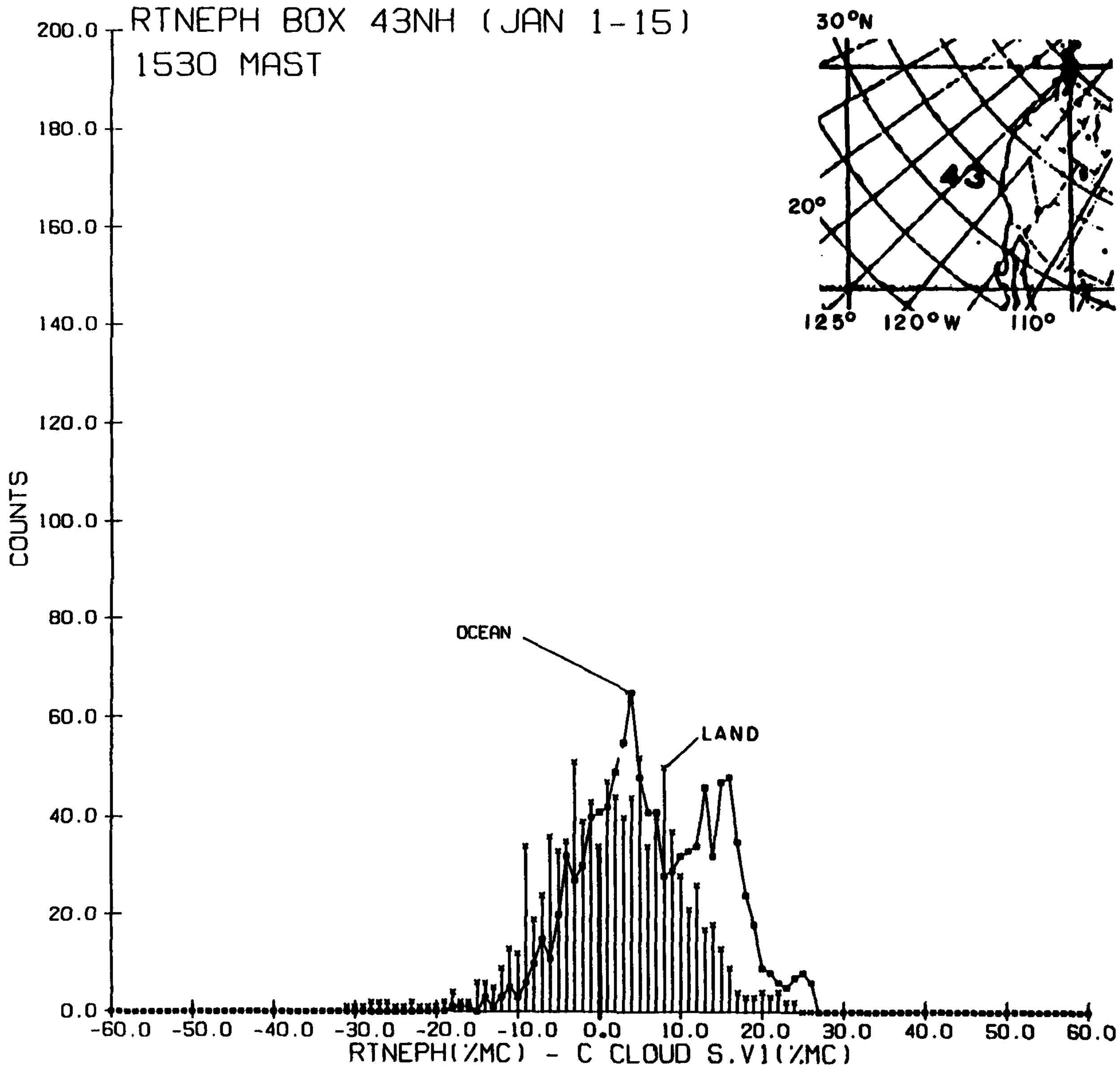

Figure 4. Counts of Percent Mean Cloud Cover (%MC) for Jan. 1-15 RTNEPH TCHT Data Minus C Cloud S Indicated Percent Mean Cloud Cover Over Land Versus Those Over the Adjacent Ocean Area for Region 43 East of 125 Degs West.

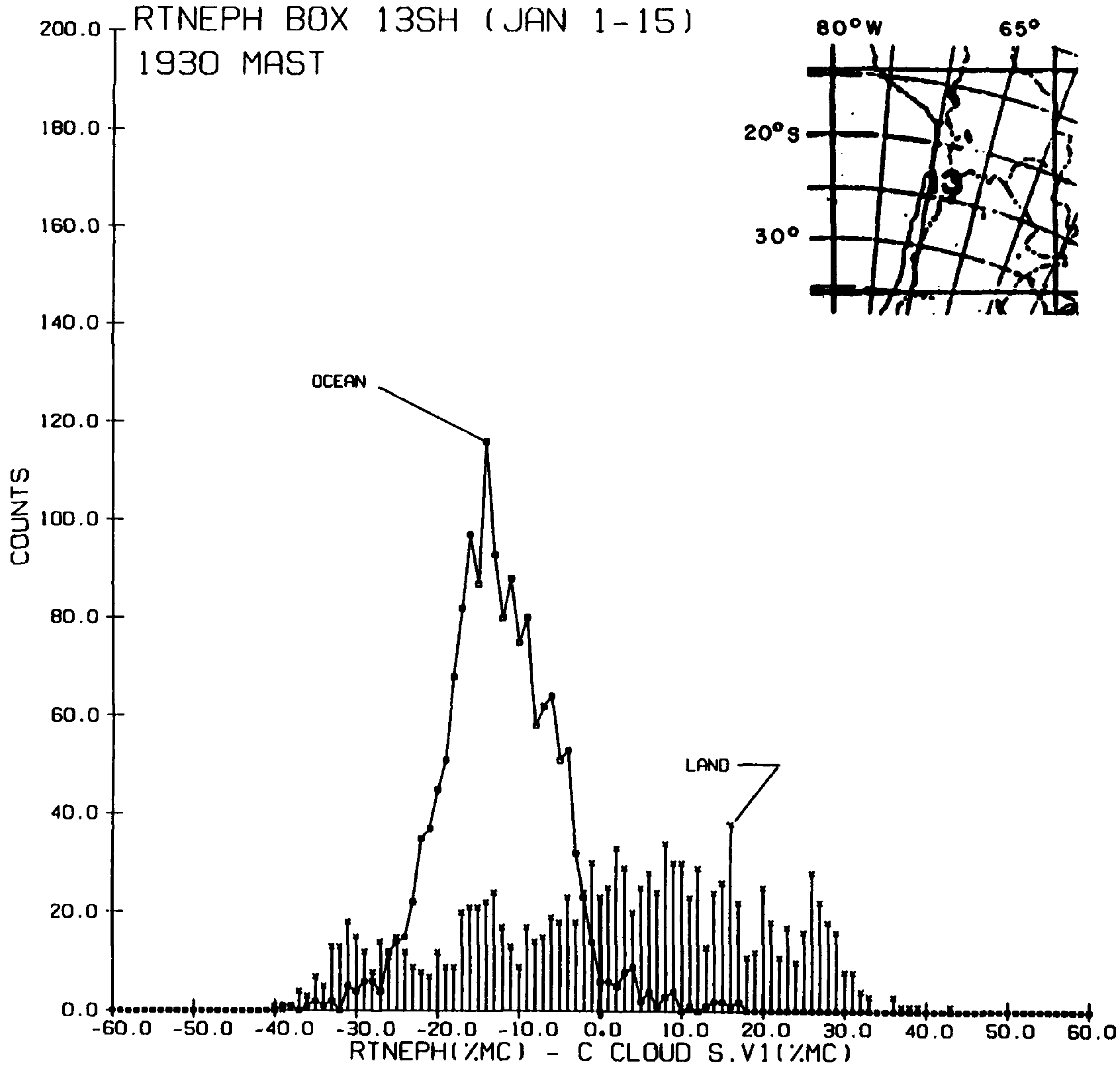

Figure 5. Counts of Percent Mean Cloud Cover (%MC) for Jan. 1-15 RTNEPH TCHT Data Minus C Cloud S Indicated Percent Mean Cloud Cover Over Land Versus Those Over the Adjacent Ocean Area for SH Region 13 West of 65 Degs West.

The Figure 4 case over the west coast of the US and the bordering Pacific Ocean shows that differences between cloud amounts from RTNEPH minus the C Cloud S indicated amounts are about the same for both land and ocean conditions, although larger cloud amounts from the RTNEPH data occur slightly more often over the ocean.

The case in Figure 5 over the South American Andes Mountains in Chile and the adjacent Pacific ocean to the west is the most interesting case. Here, most all RTNEPH amounts found over the ocean are less than indicated cloud amounts. However, differences over land vary from as much as minus 30 to plus 30 percent cloud cover.

3.2 Probability of Upslope (PUPS)

Since clouds tend to form in areas of rising air currents, we conducted an experiment to correlate upslope probabilities with differences in mean RTNEPH (TCHT) amounts and C Cloud S indicated cloud amounts. The geometry of the problem of computing upslope probabilities is shown in Figure 6.

The steps below outline the methods used to compute upslope probability (P_r) given positions and four different heights of surrounding RTNEPH small boxes and vector mean wind components at 500 millibars.

First, the global wind vector components $\bar{u}$,$\bar{v}$, and standard deviation of $\bar{u}$ (S_u) and $\bar{v}$ (S_v) from the ECMWF 500 MB data for a given month and chosen large RTNEPH box area are retrieved. Adjustments to the vector and univariate standard deviations are then accomplished using 8 below.

$$\begin{aligned} \sigma_v &= \sqrt{S_u^2 + S_v^2} \\ \sigma &= \sigma_v \sqrt{2} \end{aligned} \qquad (8)$$

Here, σ_v is the vector standard deviation and σ is the univariate standard deviation. (See Guide for Applied Climatology, 1977).

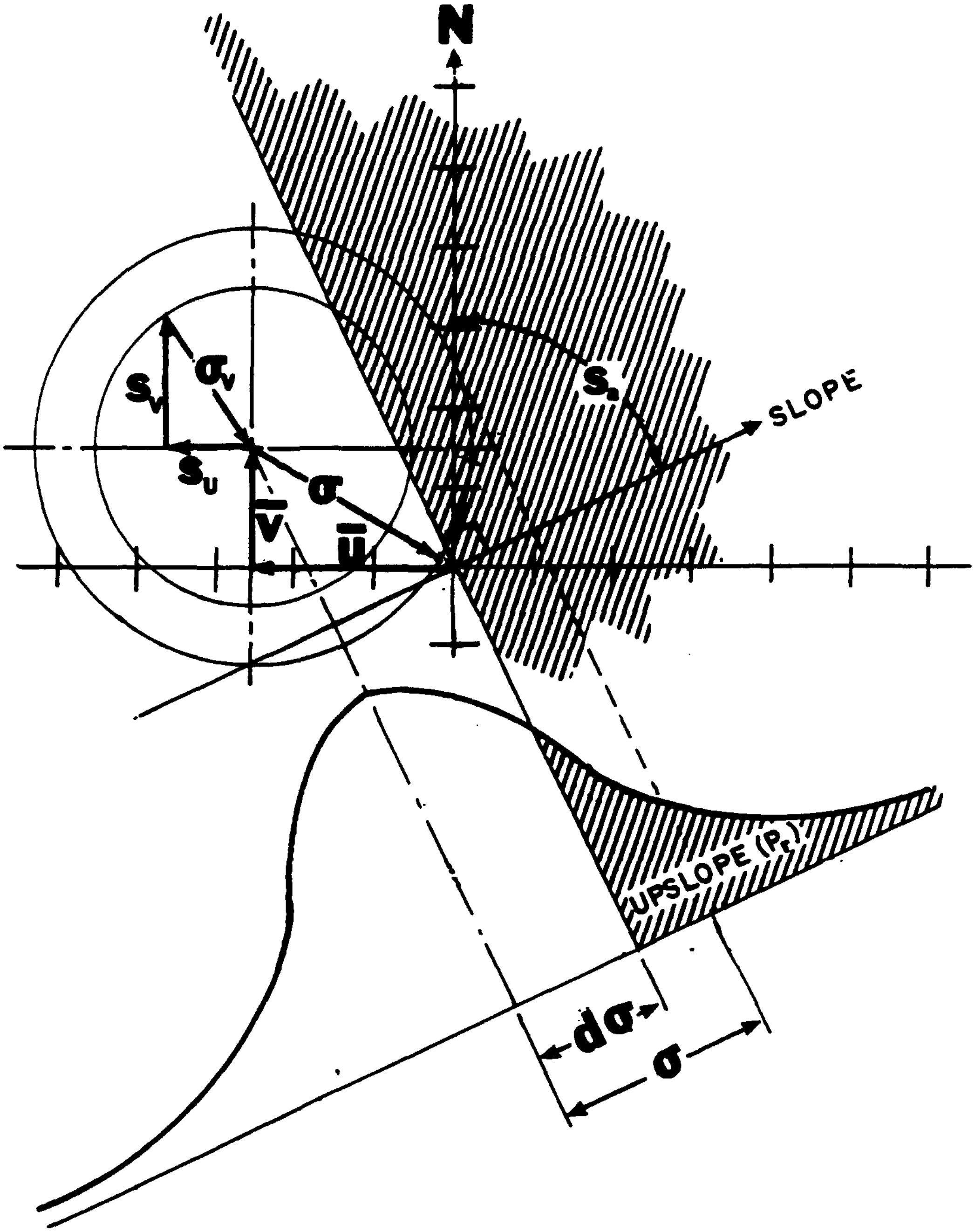

Figure 6. Geometry of the Problem of Computing Upslope Probability Given the Vector Mean Wind Components $\bar{U}$, $\bar{V}$ and Standard Deviations S_u and S_v. Probability of Upslope P_r is Obtained Knowing the Standardized Distance $d\sigma$ Along the x Axis of the Univariate Normal Distribution. This Distance is Governed by the Perpendicular to the Line of the Azimuth Angle S_a of the Slope of the Terrain of a Given RTNEPH Box.

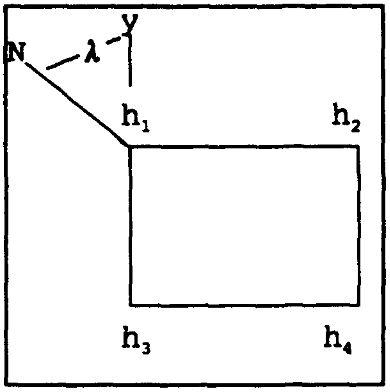

Figure 7.

Next, we use bilinear interpolation to get values of $\bar{u},\bar{v}$, and σ at the center of each small RTNEPH box. Moreover, the center box of interest is rotated by a certain number of degrees, with the number depending on its longitude for box orientation northward, angle γ in Figure 7. The slope of the RTNEPH box in question is computed using the heights of surrounding boxes. Thus, heights h are oriented like those shown to the left where h equals height in meters at surrounding box locations 1,2,3, and 4. Now the slope of the box in question can be computed from the equations

$$S_x = \frac{(h_2 - h_1) + (h_4 - h_3)}{2} \quad . . . . \quad (9)$$

and

$$S_y = \frac{(h_1 - h_3) + (h_2 - h_4)}{2} \quad . . . . \quad (10)$$

The angular slope ζ of the box is

$$\zeta = \tan^{-1}\left[\frac{S_y}{S_x}\right], \quad . . . . \quad (11)$$

where the correct quadrant is chosen by the FORTRAN routine ATAN2. The azimuthal S_a (upslope direction) is

$$S_a = \zeta - \lambda \, , \quad . . . . \quad (12)$$

where λ is the orientation of the RTNEPH box with respect to north.

Next, standardized distance d as an equivalent normal deviate,

END, is computed from the equation

$$d = \frac{1}{\sigma}\left[\,\overline{u}\cos(S_a) + \overline{v}\sin(S_a)\right], \quad \ldots\ldots \quad (13)$$

where $\sigma, \bar{u}, \bar{v}$, and S_a are defined above.
Finally, probability of upslope PUPS (P_r) is computed by a routine called pnorm, P_r = pnorm(d), which converts END's to probabilities.

The ranges of probabilities p are $0 \le p \le 1$ where p of 0 to .5 indicates downslope severity, .5 is a neutral slope condition, and p greater than .5 indicates upslope severity. These probabilities centered over each RTNEPH small box are stored into a 63 X 63 array for comparison with cloud amount differences between RTNEPH and C Cloud S.

3.2.1 Upslope Case Studies

The algorithm for computing the probability of upslope was initiated over selected case areas within the three RTNEPH large box areas numbered 13, 43 and 12. Details of the cases studied are presented in the following sections.

3.2.1.1 Chile Andes Mountain Case.(RTNEPH SH Region 13)

An area over the South American Chile Andes Mountains enclosed within a rectangle having a lower left coordinate of 23 degs south and 72 degs west and an upper right position at 19 degs south and 61 degs west (Figure 9a) was chosen to correlate probable upslope conditions with cloud amount differences between RTNEPH and C Cloud S.

From the scatter plot shown in Figure 8. it can be seen that out of 357 points (N) within the chosen area of the Chilean Andes Mountains case, correlation of PUPS with RTNEPH amounts minus indicated C Cloud S cloud amounts is rather small (CORR=.43). This rather dismal result prompted the development of additional software that was used to portray all data arrays involved in the analysis for detailed observation. Each of these arrays is presented here for discussion.

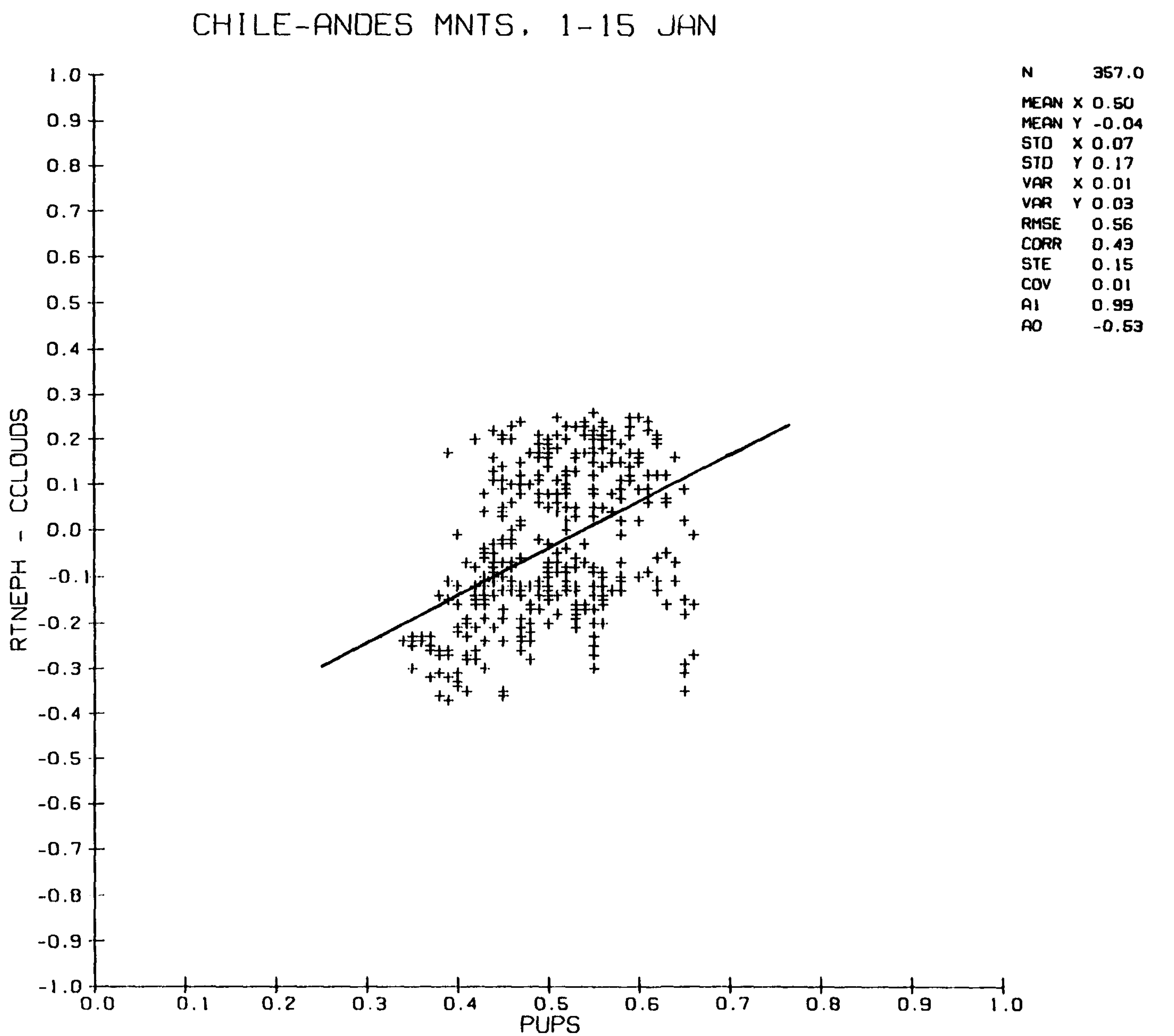

Figure 8. Scatter plot of PUPS Versus RTNEPH Amounts Minus C Cloud S Indicated Cloud Amounts for the Chile-Andes Mountain Area Outlined in Figure 9f.

Figures 9b,c,d,e, and f portray "quick" printouts of the data contents of each array used in the PUPS versus cloud amount analysis for the RTNEPH region 13 case. All of these figures represent data in each cell at the full RTNEPH small box resolution. Five degree latitude and longitude lines and coastal boundaries are overlaid for reference. The number or character shown for each cell in a display is a coded data element which can be related to the parameter boundary conditions shown in the upper right index of each figure.

Figure 9a shows a reference map of region 13. The 305 meter terrain contour is included to distinguish the higher terrain of the Andes mountains from the lower valleys in central South America.

Figure 9b portrays the C Cloud S indicated mean cloud covers (looking down) for January at 1800 MAST over the entire RTNEPH southern hemisphere region 13. Note how smooth the coded contours are that represent indicated mean cloud cover over the region. High amounts of cloud are correctly indicated over the upper right side of the area near the Amazon tropical rain forest. As expected, lower amounts of cloud are indicated over the upwelling ocean areas just off the coast of Chile on the left side of the figure. The contours of indicated cloud amounts in the figure show no indication of any mountain terrain effects on cloud amounts.

Figure 9c shows the coded mean terrain heights, altitudes, of each RTNEPH small box. The code in each cell was derived by dividing each RTNEPH small box height by the maximum height found in the area, 5151 meters in this case. This coding scheme was done only for data presentation purposes. Actual altitudes versus codes are shown in the index to the upper right side of the figure. Dots and hats codes are meant to enhance the appearance of the highest values within a figure for ease in comparison with other parameters.

Figure 9d shows the mean RTNEPH amounts in each cell as computed from the TCHT histogram data (Section 2.1.2).

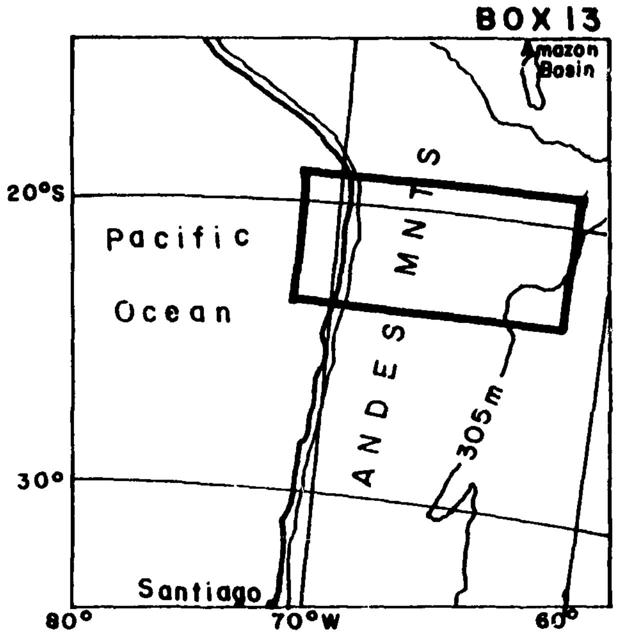

Figure 9a. Reference Map of RTNEPH Southern Hemisphere Box Number 13.

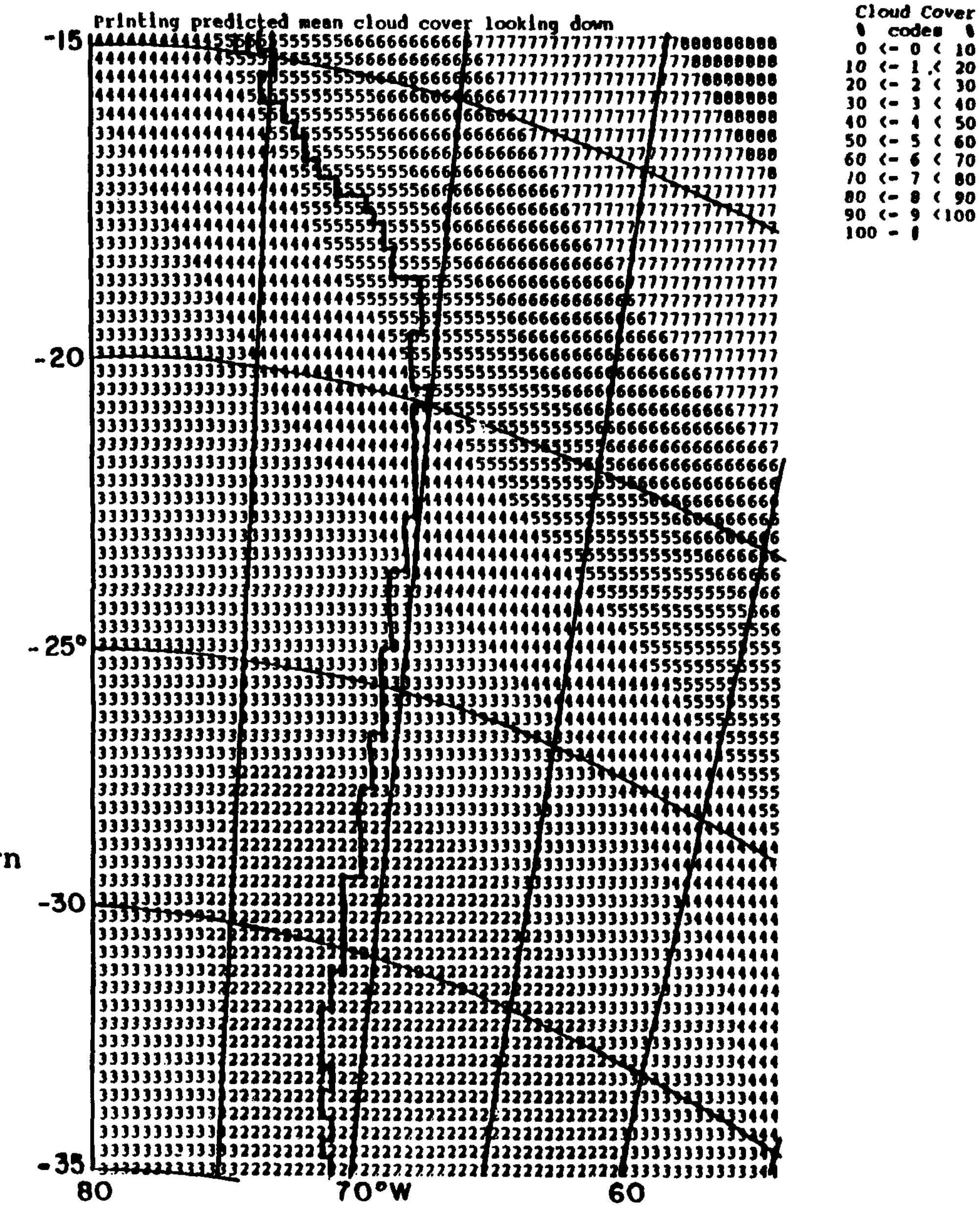

Figure 9b. Indicated Cloud Amounts.

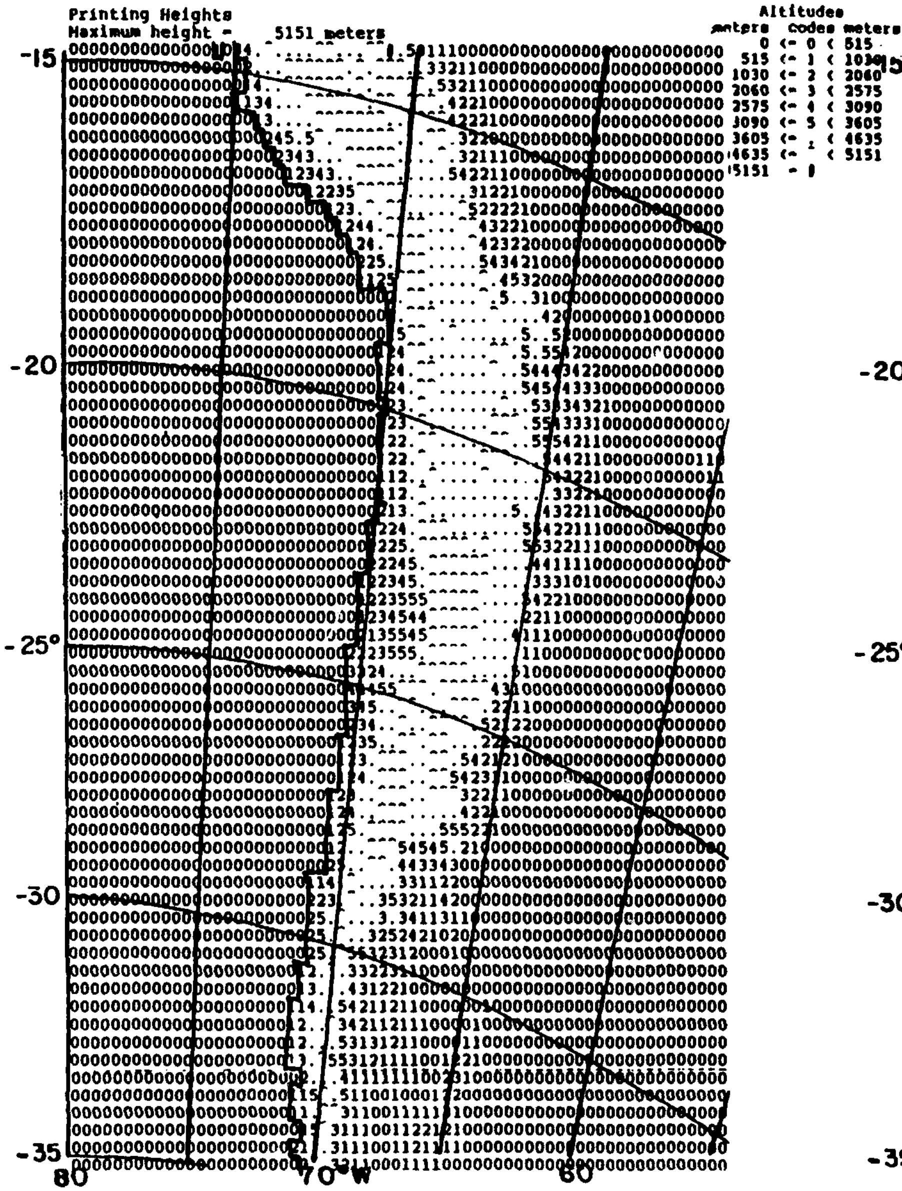

Figure 9c. Altitudes.

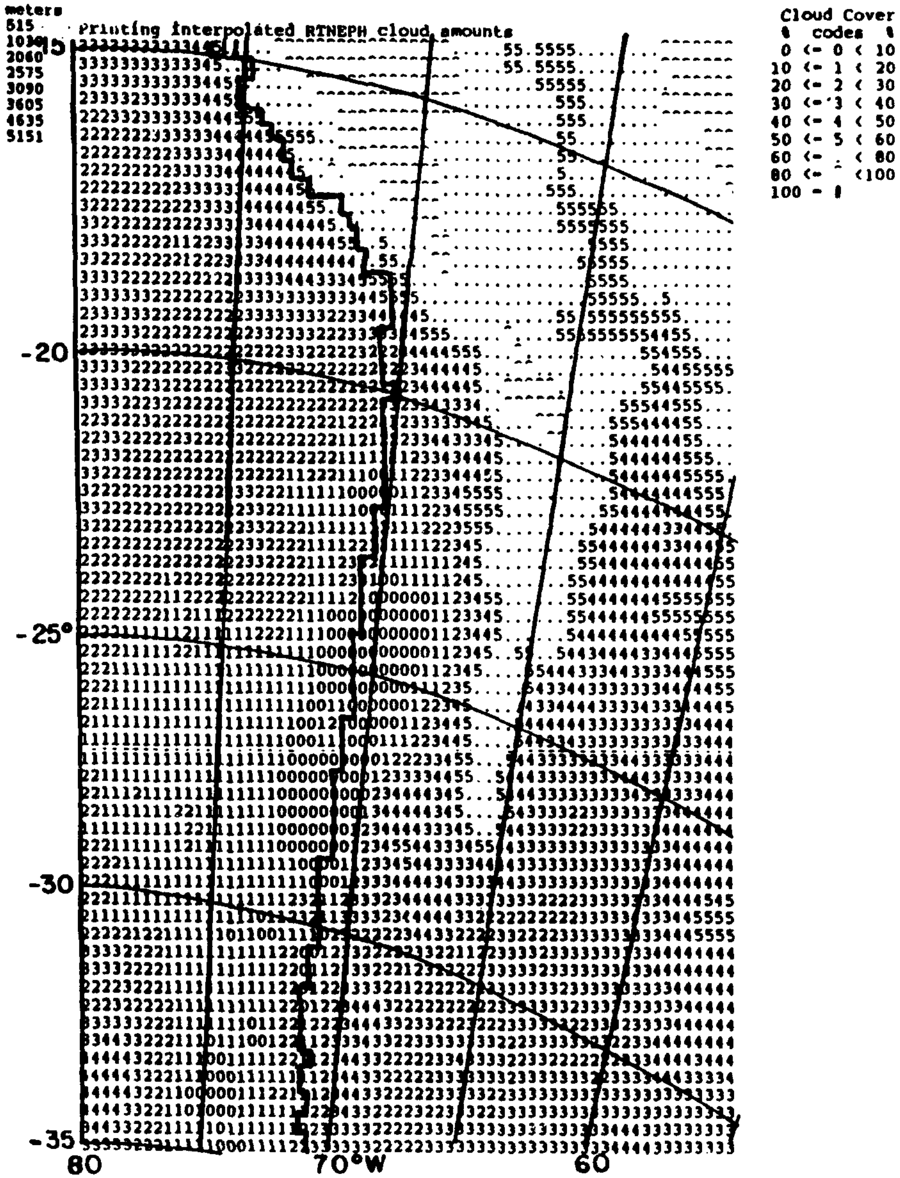

Figure 9d. RTNEPH Amounts.

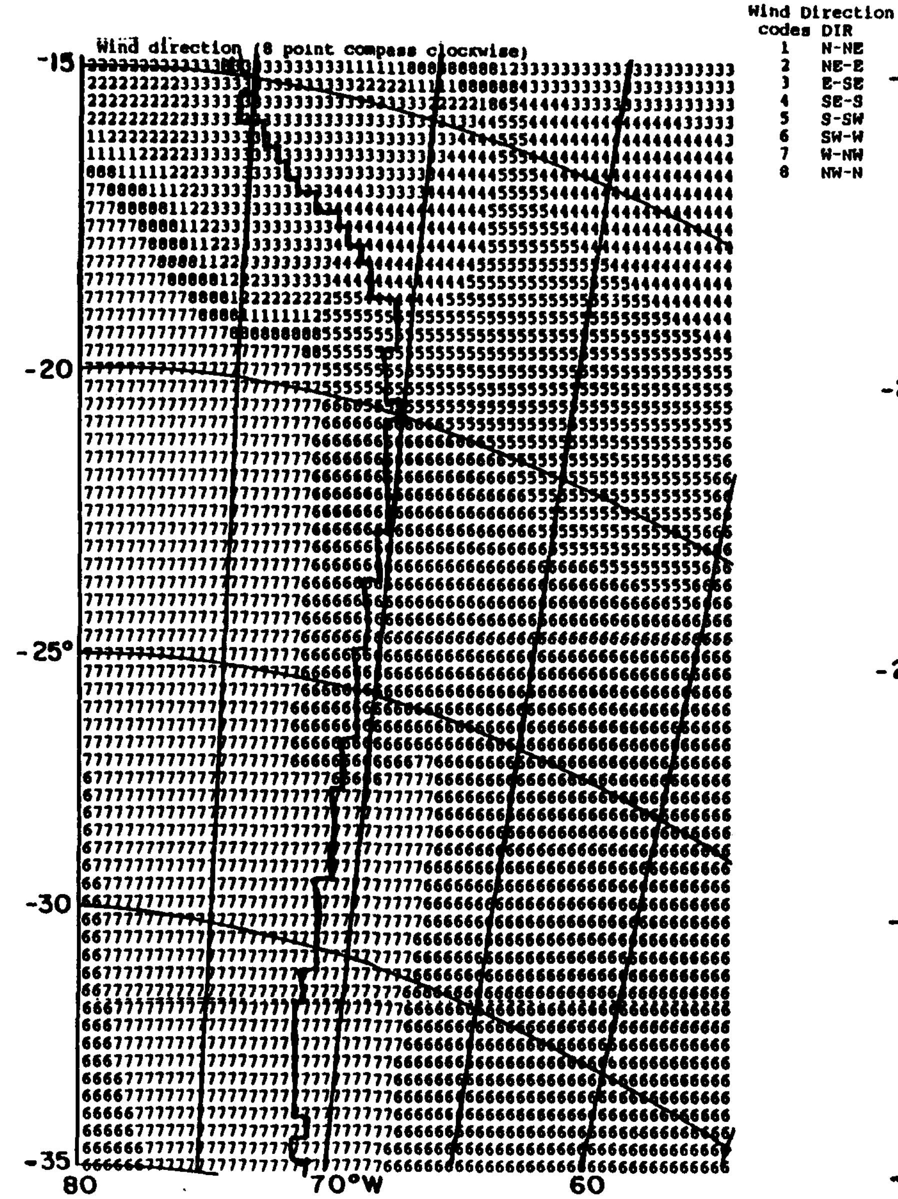

Figure 9e. Vector Mean Wind Directions.

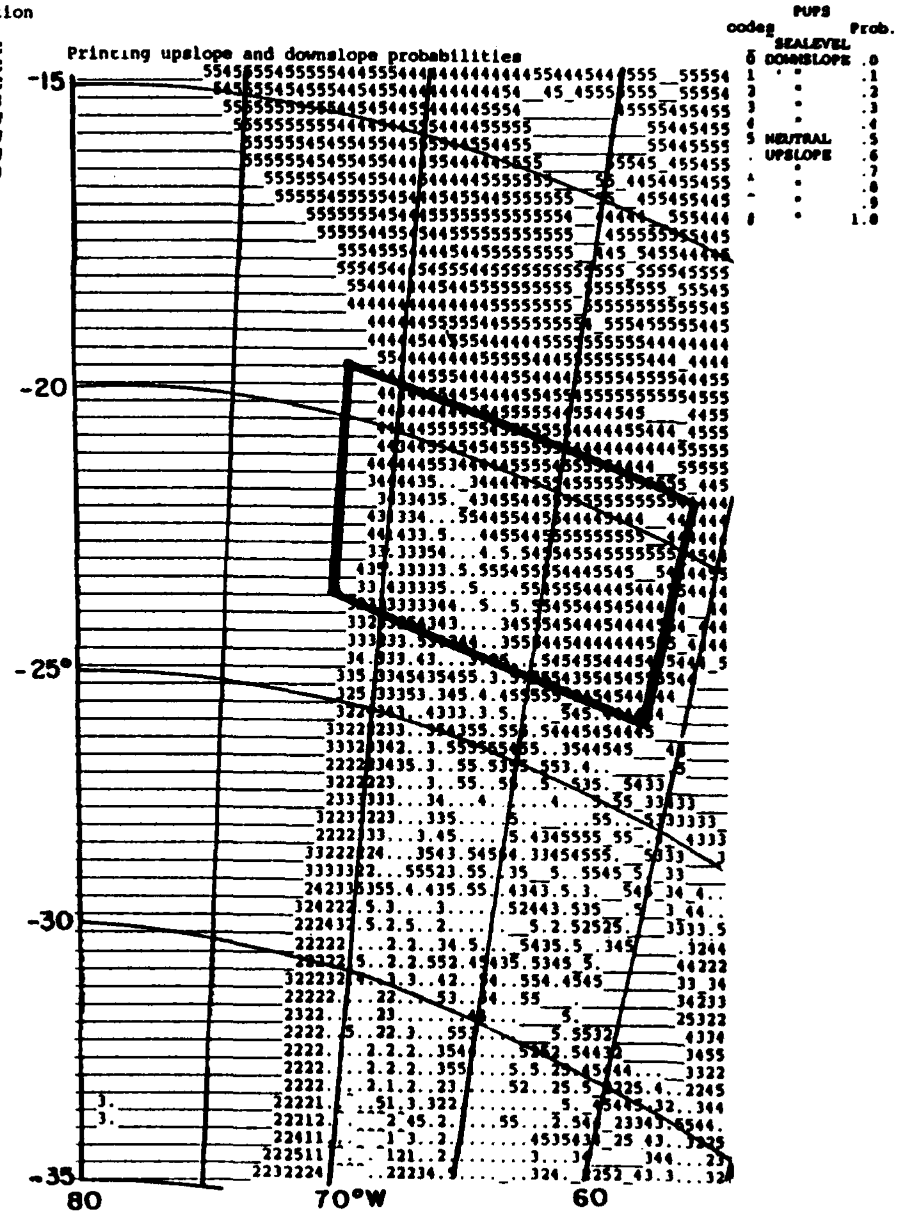

Figure 9f. Upslope Probabilities.

Figure 9e displays coded vector mean wind directions d_v which were computed by (14) below using the $\bar{u}$ and $\bar{v}$ wind components found in the ECMWF database for January at the 500 millibar level.

$$d_v = \frac{\pi}{180} \tan^{-1}\left[\frac{\bar{v}}{\bar{u}}\right] \quad \ldots\ldots\ldots\ldots \quad (14)$$

The codes shown are for the wind direction quadrants listed in the upper right hand side of the figure. For example, code 7 represents a mean wind direction component that is <u>from</u> the west to northwest quadrant.

Figure 9f shows upslope probabilities (PUPS) that are calculated for each small RTNEPH box in region 13. The horizontal lines (underscores) in this figure signify RTNEPH small box heights near sea level or boxes that are parts of plateau's and are therefore areas where PUPS were not computed. The data within the outlined area in this figure were those used to create the scatter plot in Figure 8. Note that from Figure 9e the mean 500 millibar vector wind direction components are mainly from the south and southwest quadrants. The strongest upslope probabilities in the area (Figure 9f) appear to be clustered over the highest peeks (Figure 9c), which are situated along the western side of the Andes. However, the highest mean RTNEPH cover, (Figure 9d) appears over the eastern side of the Andes mountain chain. That is, the bulk of the cloud cover is oriented in a north-south direction centered along the western meridian of 65 degrees whereas the center of the Andes Mountain chain running north to south is centered more nearly along the 67 degree meridian. We conclude then that these cloud patterns may be caused by a blocking effect. Clouds coming in from the east are blocked by the Andes mountain chain in this area, and are not the result of upslope conditions.

3.2.1.2 Cascades and San Joaquin Valley. (RTNEPH NH Region 43)

Two cases were studied over the RTNEPH NH region number 43, one over the Cascades and the other over the San Joaquin-Sierra Nevada areas.

As known, large amounts of precipitation occurs over the Cascade mountain ranges from November through April. Therefore, a small rectangular area over the Cascade range was selected to correlate possible upslope probabilities in the area with differences in cloud amounts from RTNEPH and C Cloud S. The lower and upper coordinates of the area are 44 degs north, 124 degs west and 47 degs north, 120 degs west respectively.

The scatter plot in Figure 10 shows the results of the correlation of PUPS with cloud amounts from the RTNEPH minus those from C Cloud S. The number of points N encountered in the area was 51. Again, a low correlation coefficient (CORR = .26) emerges. We therefore display all of the data arrays used in the analysis as we did with the case over the Andes Mountains.

Figure 11a is an enlarged portion of RTNEPH box number 43 showing the west coast of the United States and the outlined areas of study. Also shown in the figure is the 305 meter contour that separates lower terrain levels from the higher levels of the Cascade and Sierra Nevada mountain ranges.

Figure 11b shows indicated mean cloud cover amounts over the entire RTNEPH box number 43 for January at 1500 MAST. As expected, high amounts of cloud (70%) are predicted just off the northwestern coast of the United States. Cloud amounts then steadily decrease southward to Baja California where mean cloud amounts are about 30%. Nowhere within the figure is there any indication of small scale terrain induced cloud effects.

Figure 11c portrays coded altitudes over the entire area where codes were derived by dividing altitudes in each cell by the maximum mean altitude in the area, 3298 meters. Actual altitudes versus codes are shown in the index to the upper right side of the figure.

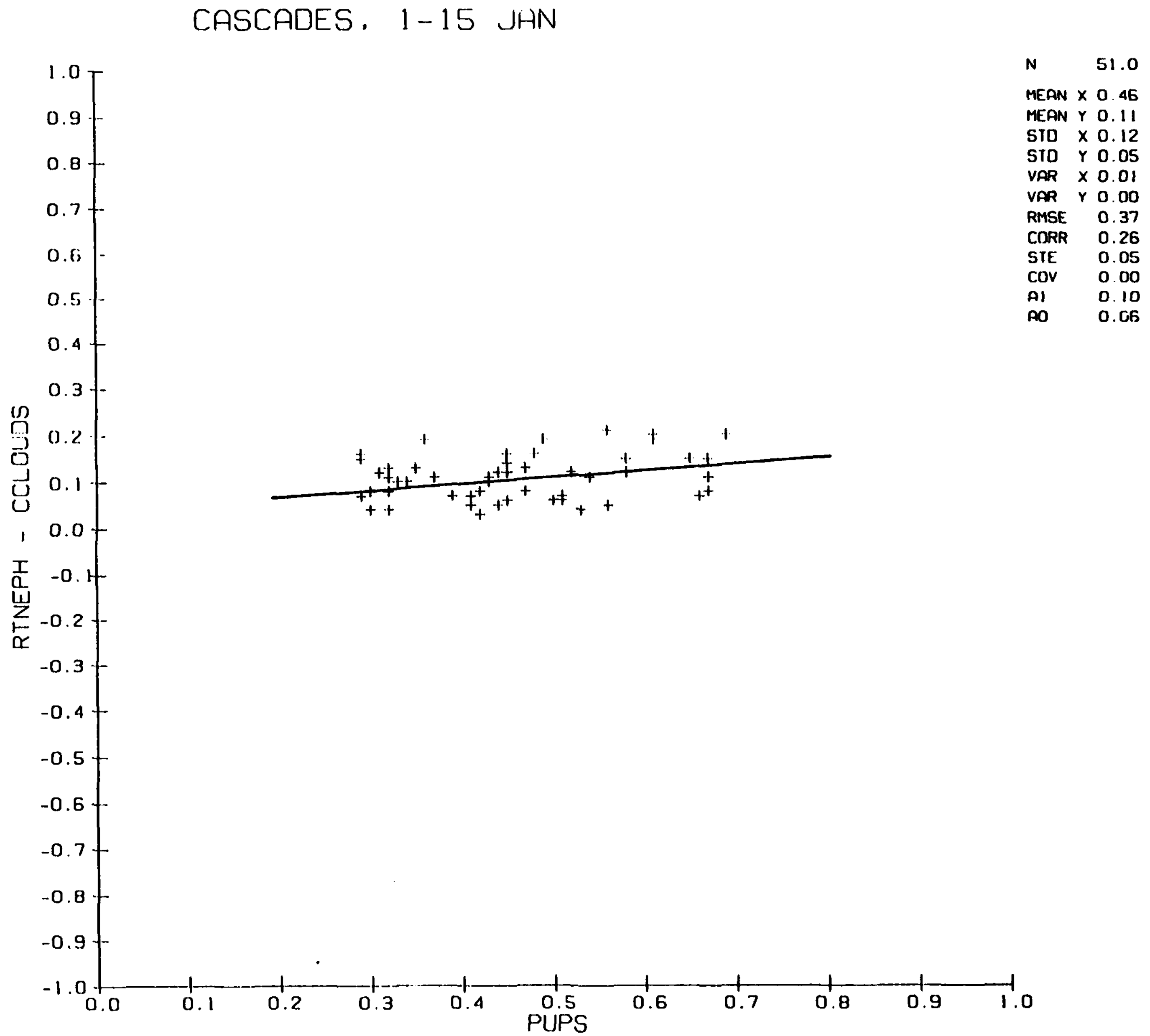

Figure 10. Scatter plot of PUPS Versus RTNEPH Amounts Minus C Cloud S Indicated Cloud Amounts for the Cascades Mountain Area Outlined in Figure 11a.

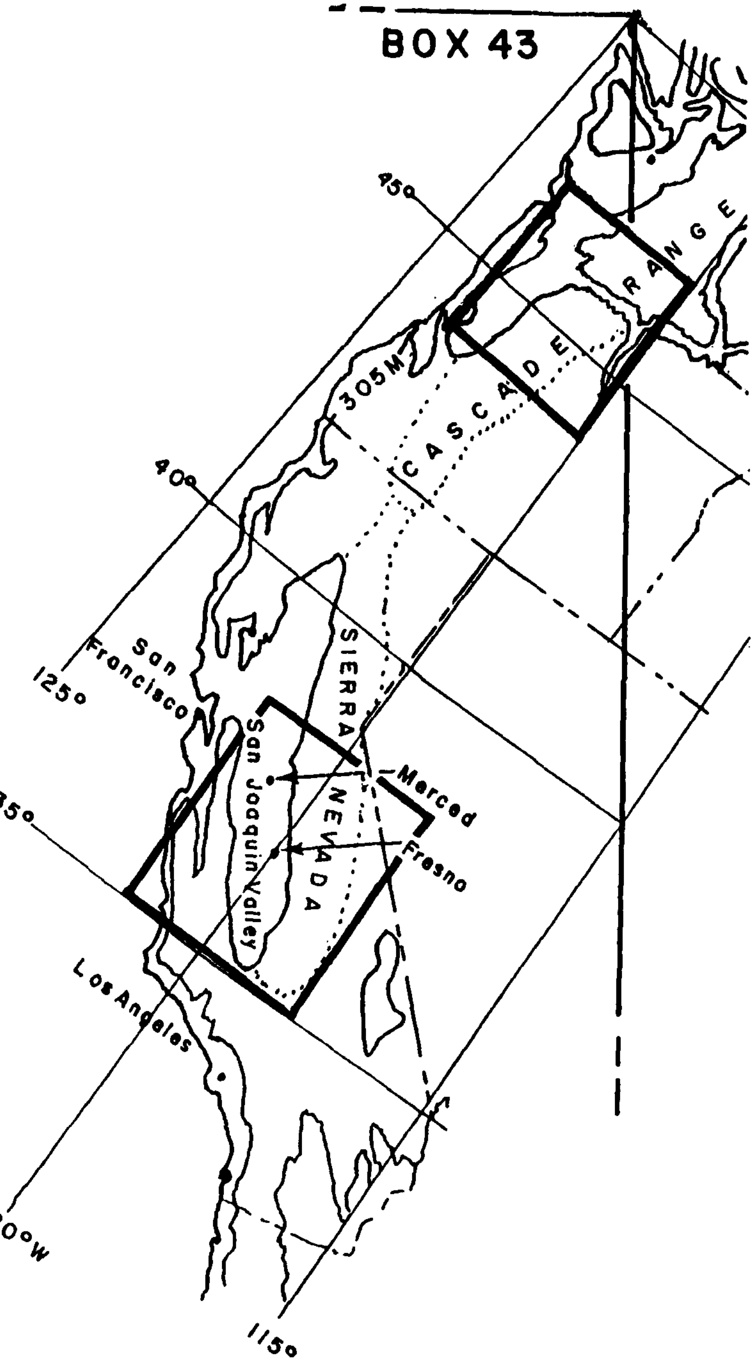

Figure 11a. Reference Map of RTNEPH Northern Hemisphere Box Number 43.

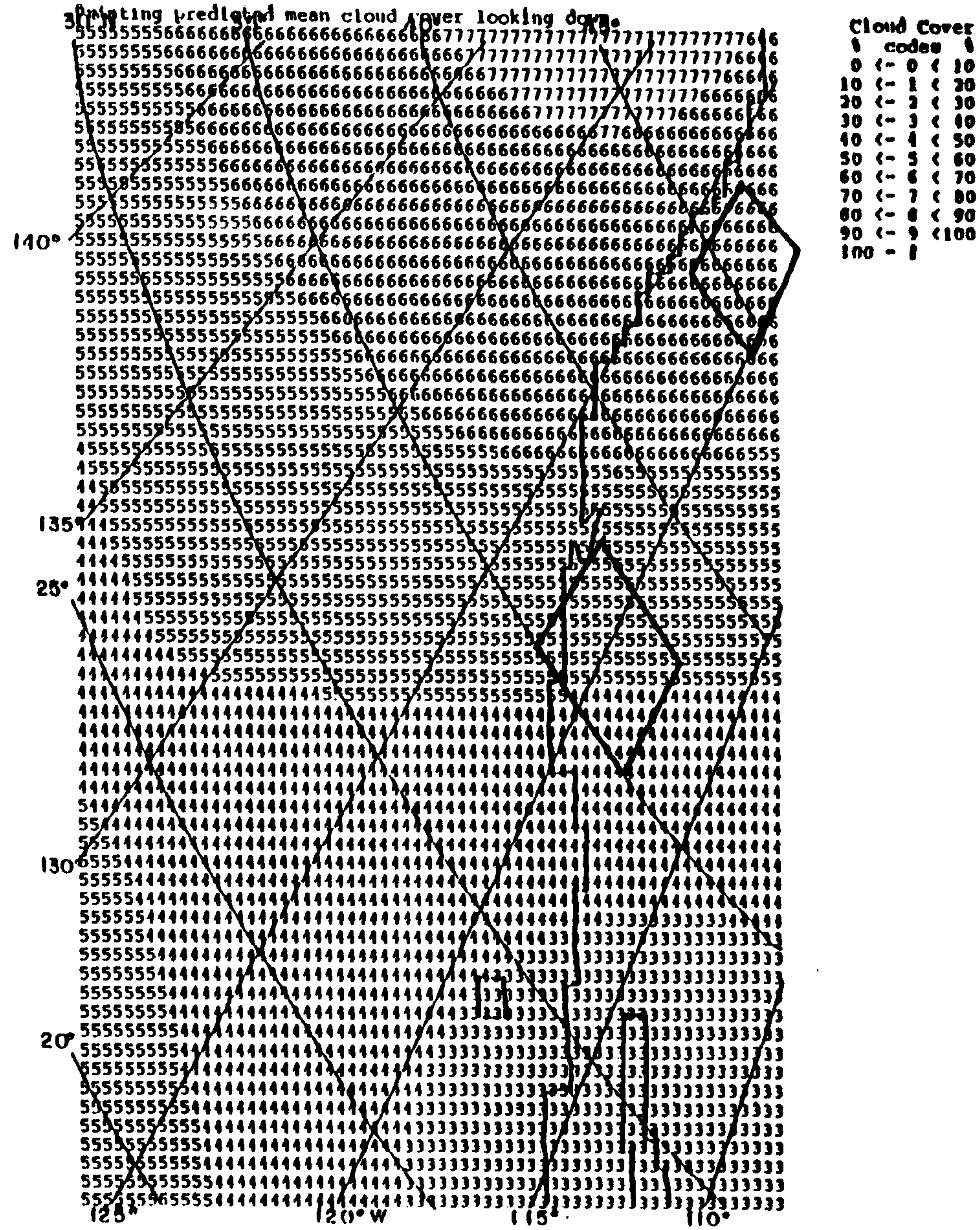

Figure 11b. Indicated Cloud Amounts.

Figure 11d shows mean RTNEPH amounts computed from the TCHT data for 1-15 January.

Figure 11e and f show coded vector mean wind direction and upslope probabilities respectively.

Upslope probabilities shown within the outlined area over the Cascades in Figure 11f are not very high despite winds that are predominantly from the west (Figure 11e). Cloud amounts over the region (Figure 11d) are high, between 60% and 100%. However, so are the cloud amounts over the surrounding areas. It is therefore concluded that even if strong upslope wind conditions caused cloud development, the effects on cloud correlation analysis would be smothered because of the canopy of persistent cloudiness already spread over the entire area in the winter north of about 40 degrees north.

Figure 12 shows the scattergram of PUPS versus RTNEPH amounts minus C Cloud S indicated cloud amounts derived from the data within the area outlined over the San Joaquin Valley, Figure 11a. Again a very small correlation coefficient emerges (CORR=-.11). We therefore return to Figures 11b through f to show some interesting phenomena occurring within the valley area.

It can be seen from Figure 11c that the maximum terrain heights in box 43 are situated in the Sierra Nevada mountain chain that defines the eastern wall of the San Joaquin Valley. The highest mean altitude is 3298 meters, which occurs in the outlined area bordering 38 degrees north. Figure 11d shows a tongue of high RTNEPH amounts (60% to 80%) that extend from about 38 degs north and 122 degs west southeastward to 35 degs north. This orientation places the persistent cloudiness within the San Joaquin Valley. Going to Figure 11f, the higher probabilities of upslope within the area also appear to be located directly within the valley. Predominant winds in the area are from the west to north west quadrant, (Figure 11e).

Actual values for RTNEPH amounts, C Cloud S indicated cloud amounts, probabilities of upslope, and heights were printed out for the valley area and analyzed in detail. All of these data

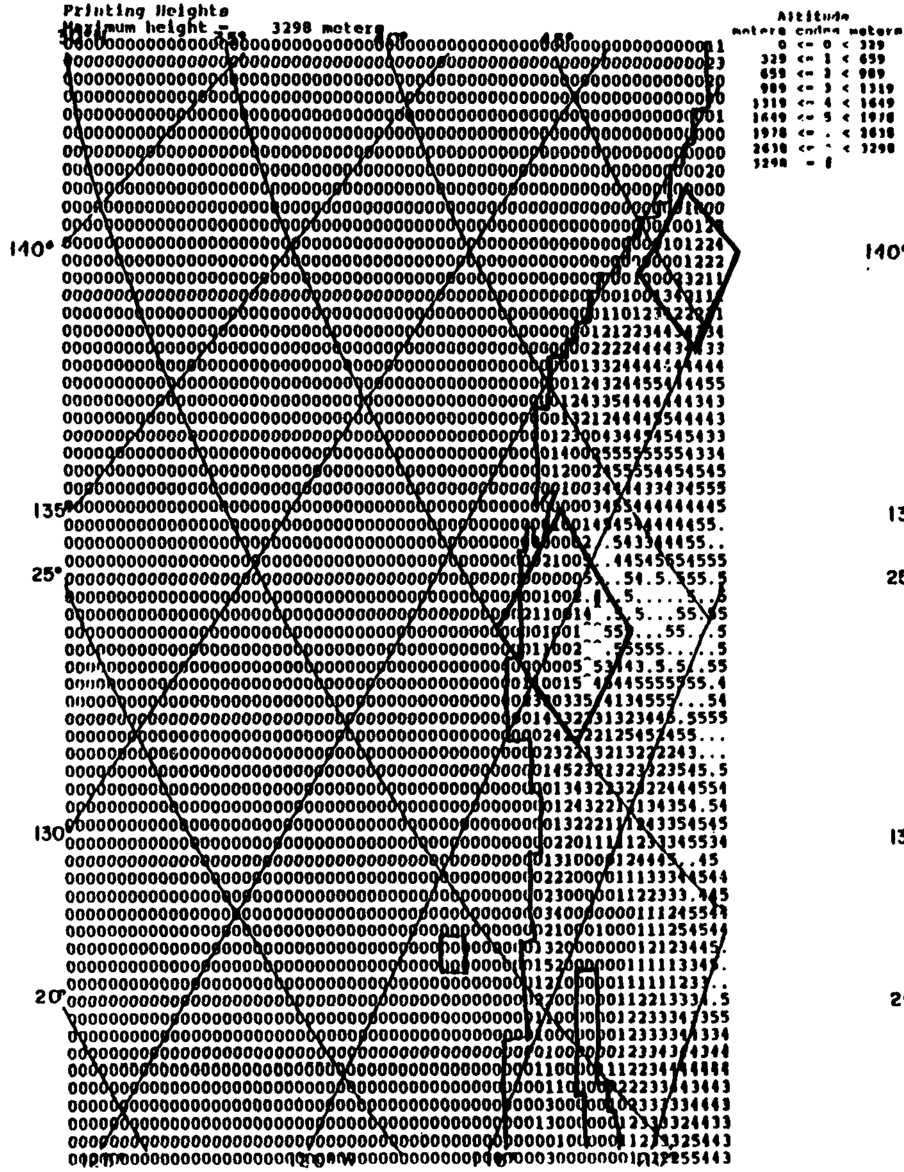

Figure 11c. Altitudes.

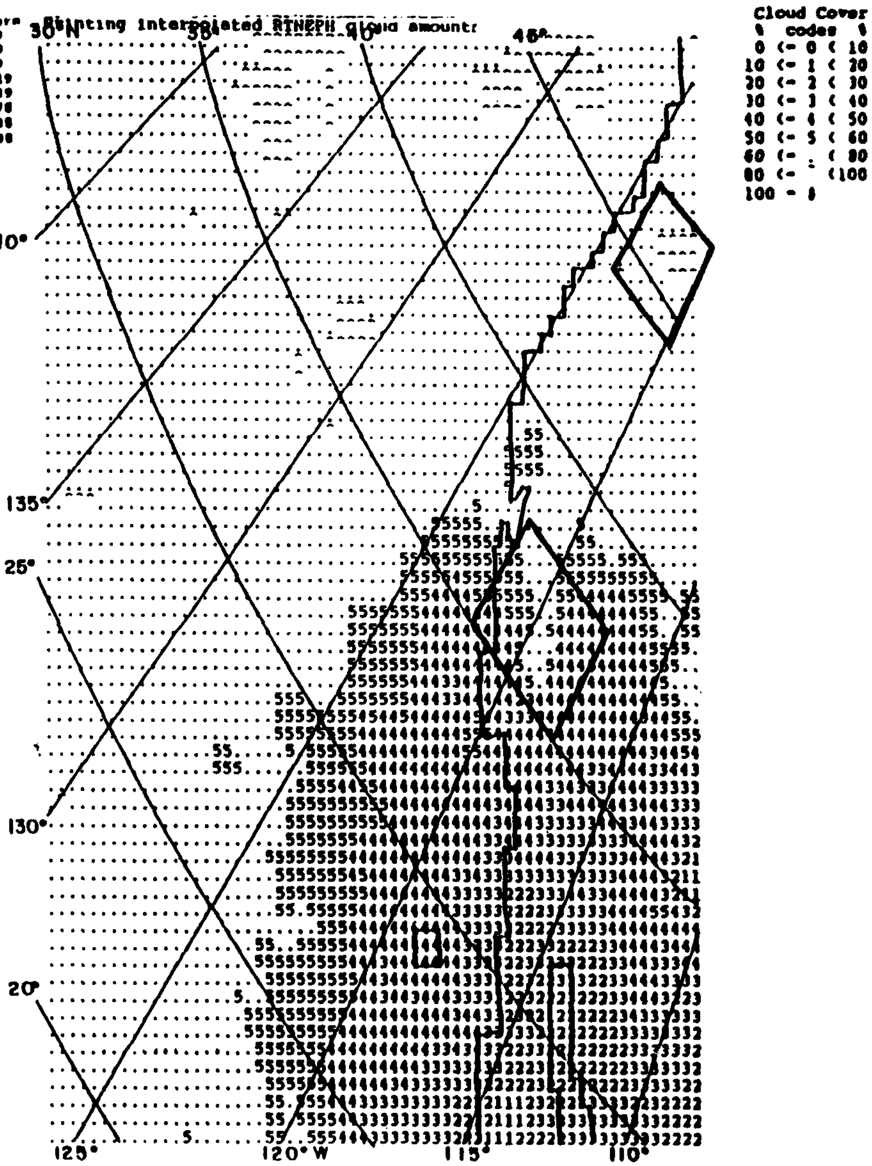

Figure 11d. RTNEPH Amounts.

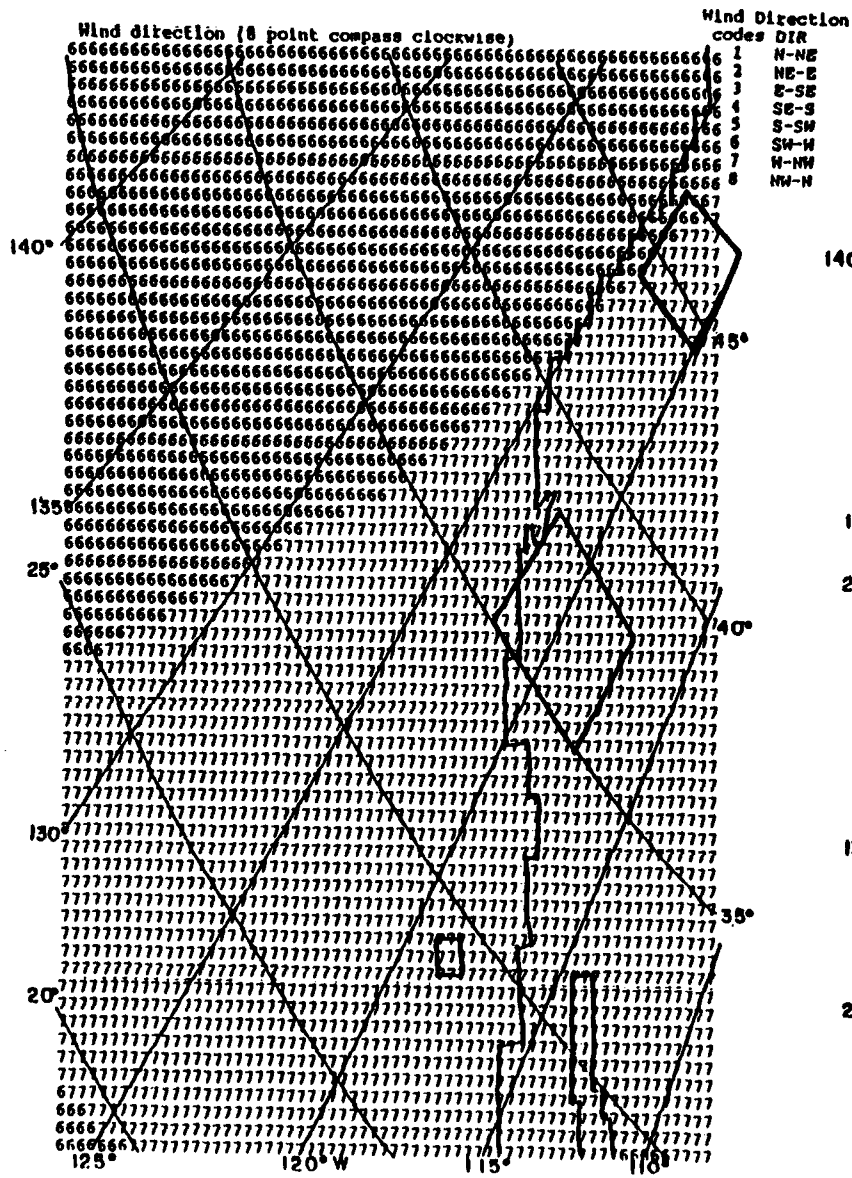

Figure 11e. Vector Mean Wind Directions.

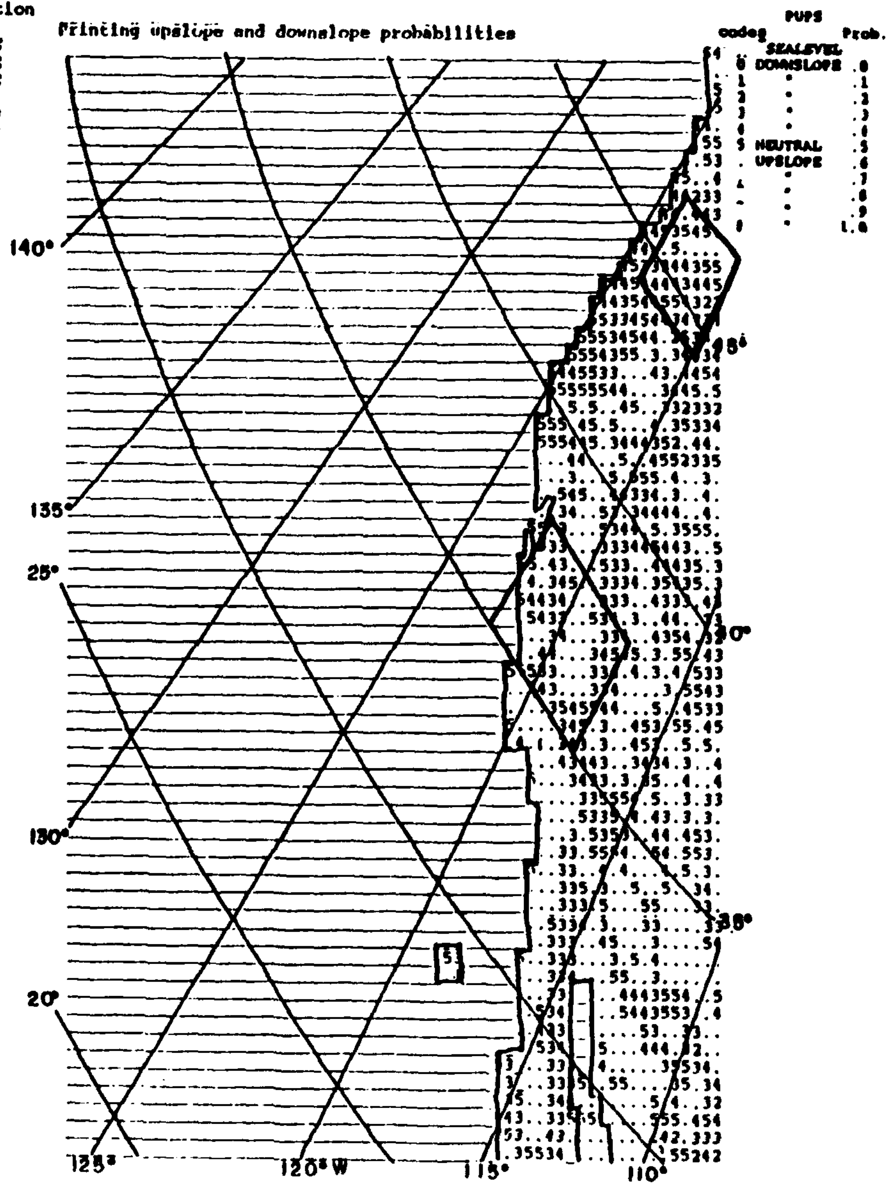

Figure 11f. Upslope Probabilities.

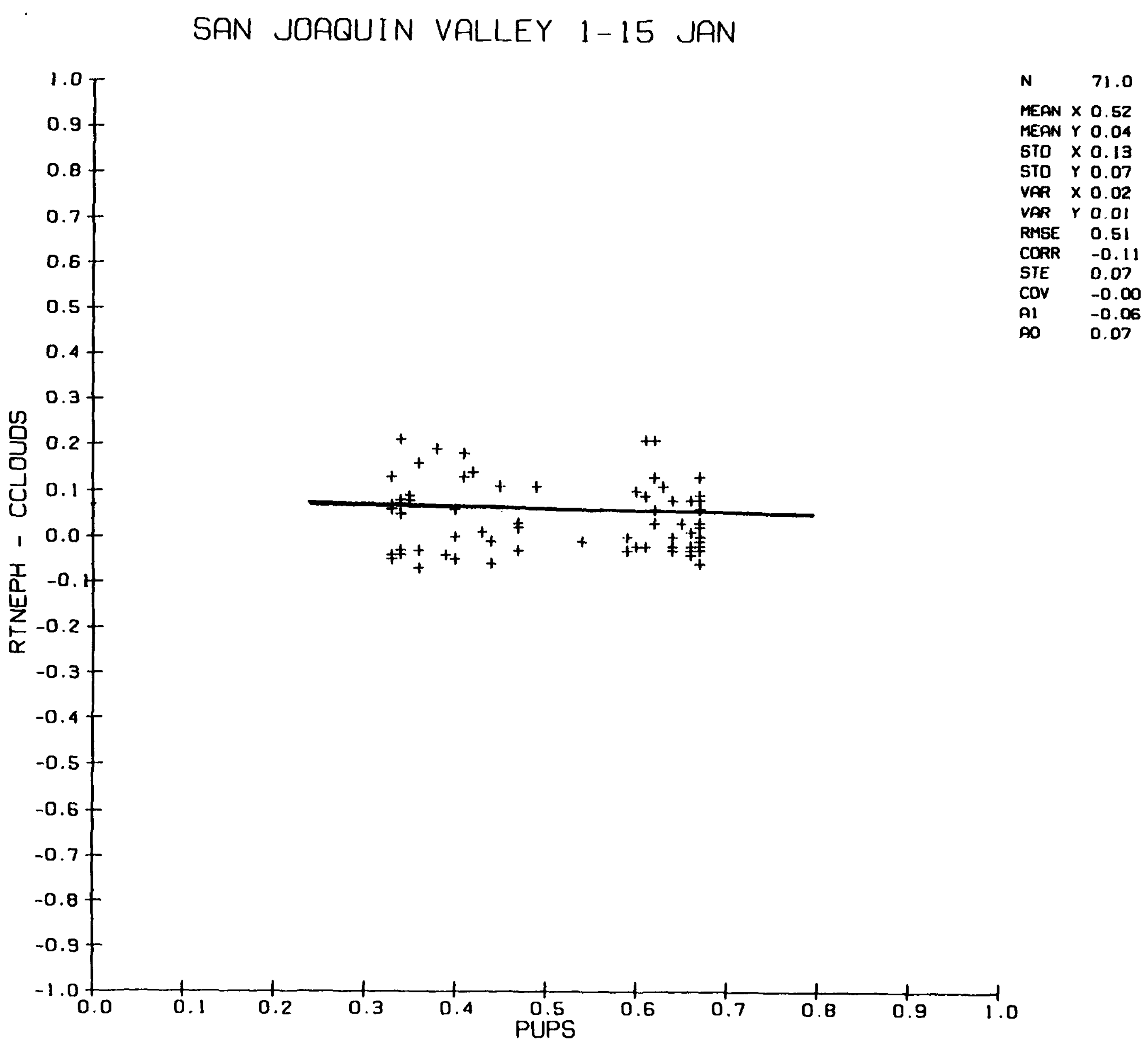

Figure 12. Scatter plot of PUPS Versus RTNEPH Amounts Minus C Cloud S Indicated Cloud Amounts for the San Joaquin Valley Area Outlined in Figure 11a.

values within the cells (footprints) along the RTNEPH map row number 355 which crosses over the southern portion of the San Joaquin Valley (bottom of Figure 13) were plotted and displayed in cross section form at the top of Figure 13. From the cross section it can be seen that high upslope probabilities and RTNEPH amounts are located within the lower terrain floor area of the valley. It is again concluded that what appears to be terrain induced cloud effects are actually caused by blockage or entrapment and not by upslope flow.

Climatological summaries of over 20 years of surface observed cloud amounts (RUSSOW's) for Merced and Fresno California (Figure 11a) also show persistent cloudiness (67% and 64% at 1500 MAST) within the area for January. A maximum average cloudiness of about 71% occurs over the area around 1000 MAST. The tongue of high cloud amounts (60% to 70%) within the valley observed by the RTNEPH satellite data persisted over a period of 75 days (5 January's X 31 days). This case reveals a typical small terrain induced cloud effect that we feel should be indicated by an automated global climatology.

3.2.1.3 Taiwan (RTNEPH NH Region 12)

Figure 14 shows the scattergram of PUPS versus RTNEPH amounts minus C Cloud S indicated cloud amounts for the case over the island of Taiwan for 1-15 January at 0900 MAST. Results show no correlation (CORR = -0.00) between the two variables. As in the other cases, we display for investigation and discussion all of the data assembled for the Region 12 Taiwan case.

Figure 15a is a reference map of the RTNEPH box area number 12 oriented south (top) to north (bottom) like that in Figure 2.

Figure 15b contains the patterns of C Cloud S indicated cloud amounts over the entire area for January at 0900 MAST. Here, small cloud amounts are indicated over Thailand, situated in the upper right corner of the figure. Cloud amount then increases rather smoothly northward to about a maximum of 60% in China just east of the higher terrain which is abundant over the China Red Basin (Figure 15c). The highest elevation in the area

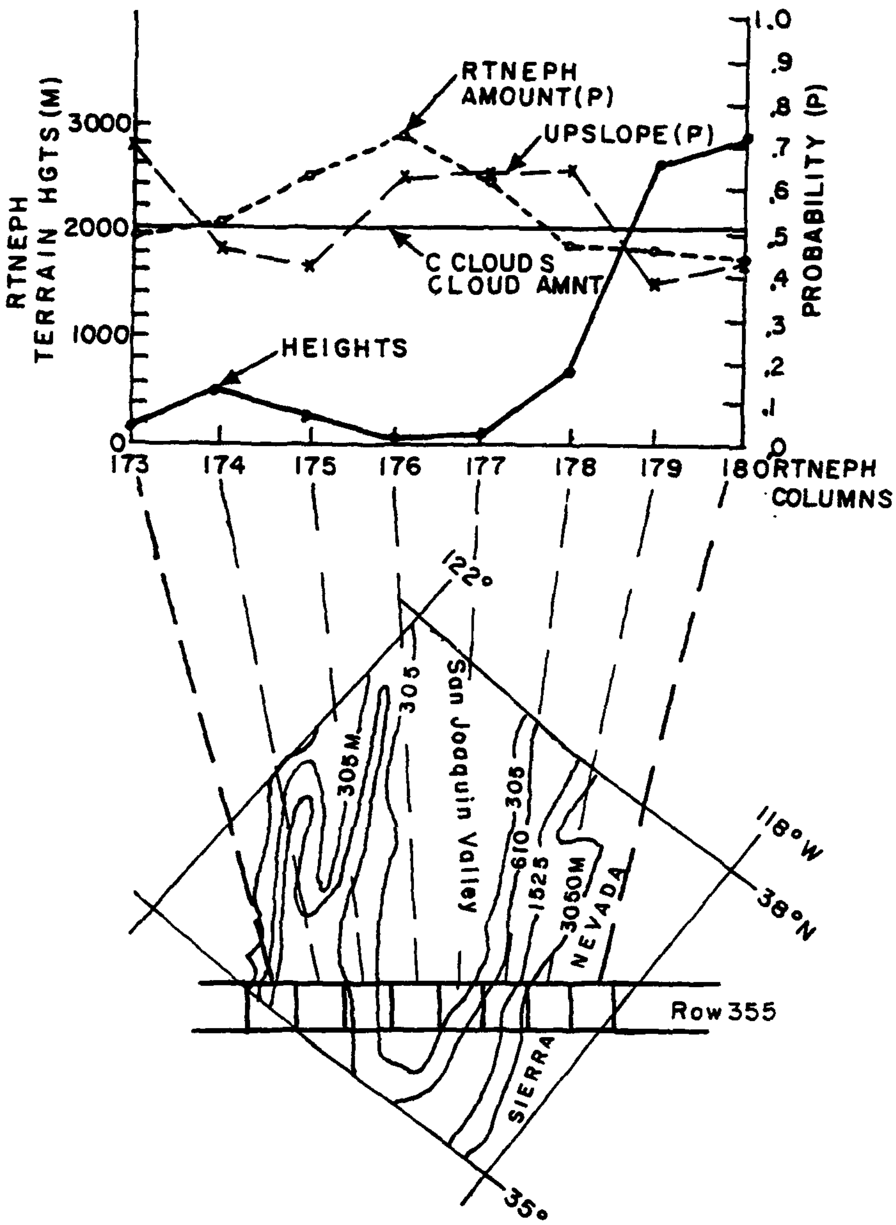

Figure 13. Four Parameters are Plotted (Top) that are Associated with the Foot Prints (Map Columns) Detailed Along the NH Map Row #355 that Crosses Over the Southern Half of the San Joaquin Valley (Bottom). The Cross Section Plots Reveal that Upslope Probabilities are Actually Higher (62% to 65%) Over the Valley than Those Over the High Sierra (About 40%). Mean RTNEPH Amounts are Also Higher in the Valley (60% to 70%) than Over the High Sierra Which Shows Only About a 45% Chance of Being Cloudy.

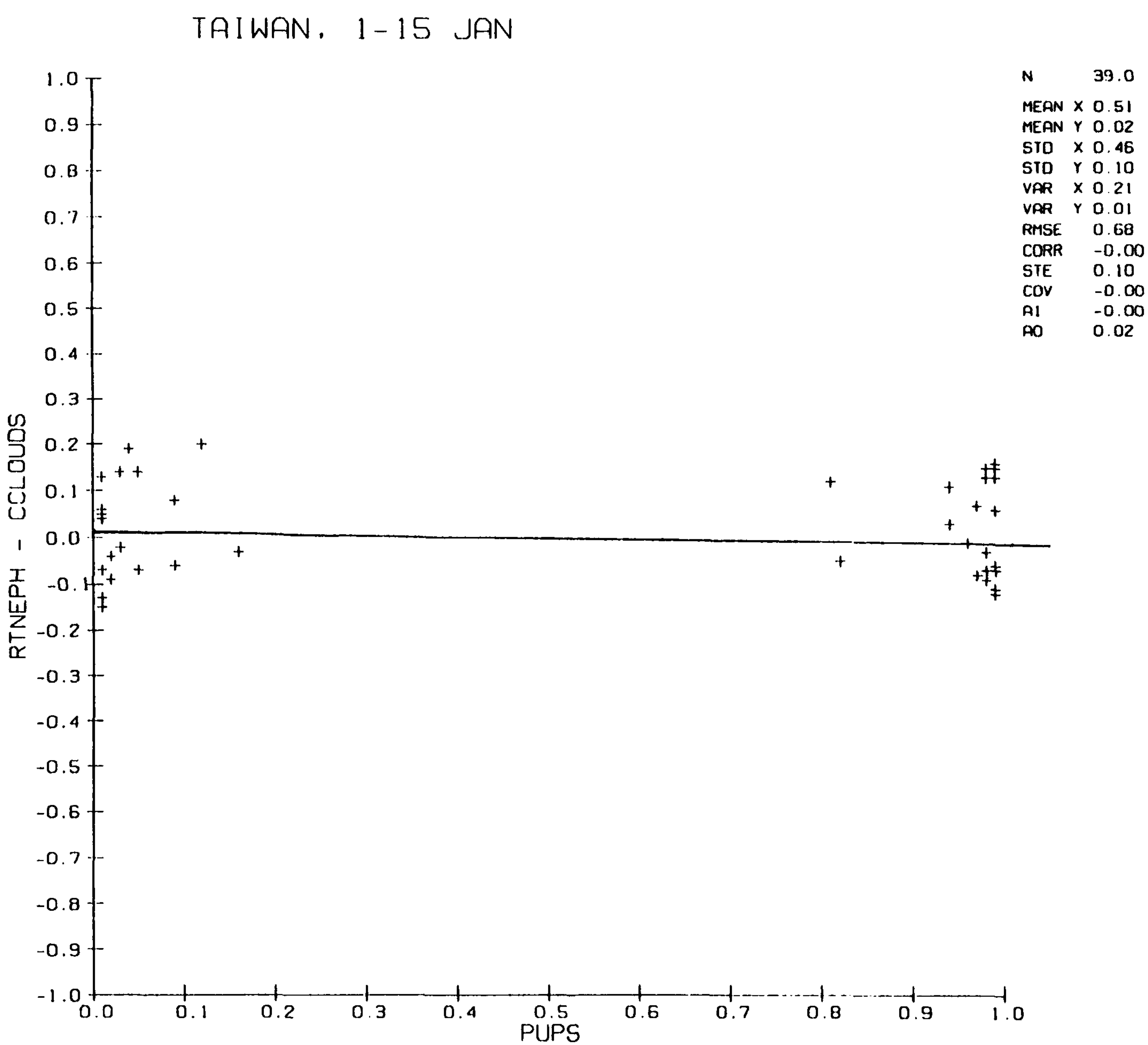

Figure 14. Scatter Plot of PUPS Vs RTNEPH Amounts Minus C Cloud S Indicated Cloud Amounts for the Taiwan Area Outlined in Figure 14b.

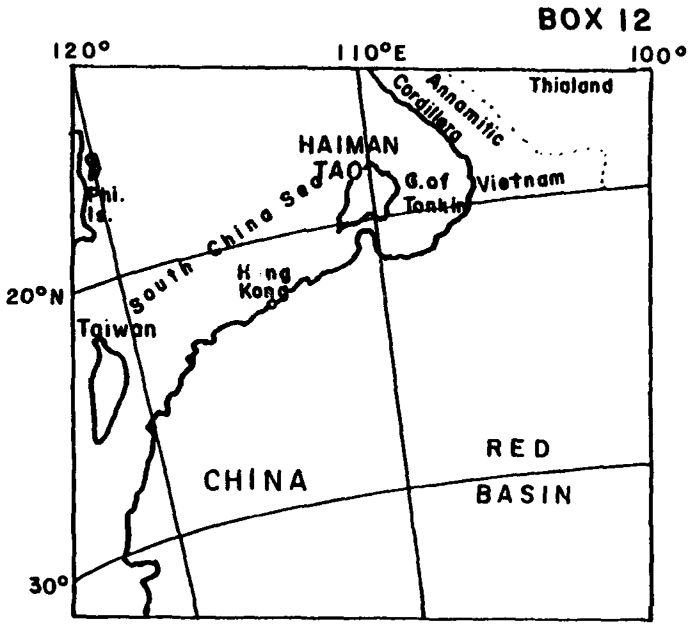

Figure 15a. Reference Map of RTNEPH Northern Hemisphere Box Number 12.

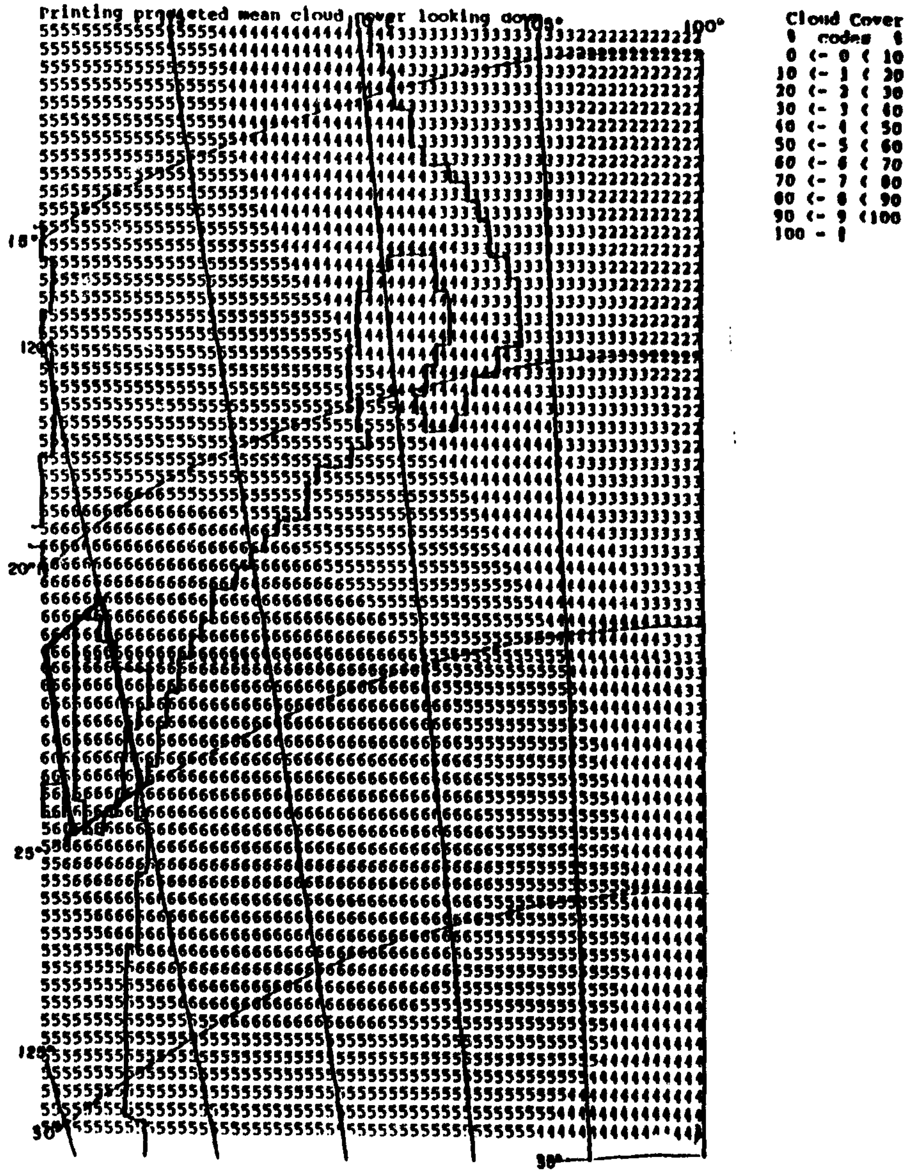

Figure 15b. Indicated Cloud Amounts.

is 4983 meters. RTNEPH amounts (Figure 15d) appear higher (80% to 100%) directly over the Red Basin. A tongue of larger amounts of cloud cover not indicated by C Cloud S can be seen stretching southward over the ocean side of the Annamitic Cordillera in Vietnam. This condition again suggests cloud build up through entrapment by a line of high terrain.

Winds at 500 MB's for the month of January appear to be mostly from the southwest to west quadrant over the entire area, (Figure 15e). Upslope probabilities (Figure 15f) are very erratic throughout the region, especially over Taiwan which is our case study area. Here, upslope probability is very high on the windward side of the island and drops off dramatically on the leeward side. This phenomenon is portrayed in detail in Figure 16. Here, four parameters associated with map columns detailed along the RTNEPH map row number 105 stretching across central Taiwan are plotted in cross section mode to facilitate analysis. The four parameters plotted are mean RTNEPH terrain heights in meters, C Cloud S indicated cloud amounts, RTNEPH amounts, and upslope probabilities. Note in particular the decrease in RTNEPH amount directly over the peak of the terrain heights near the center of the island. At this peak position the RTNEPH amounts show only about a 50% chance of being cloudy while the surrounding lower terrain areas and ocean areas show a 60% to 70% cloud amount occurrence. We conclude that for at least 50% of the time the mountains on Taiwan protrude up through the clouds below. Upslope cloud induced conditions apparently are not persistent enough to effect the climatological cloud amount conditions over Taiwan.

4. Conclusions

From the limited number of cases studied here, we conclude that differences of spatial and temporal climatological cloud cover conditions along land-sea boundaries are not significant over all areas of the world. Although the premise of using probabilities of upslopes to predict small scale cloud cover

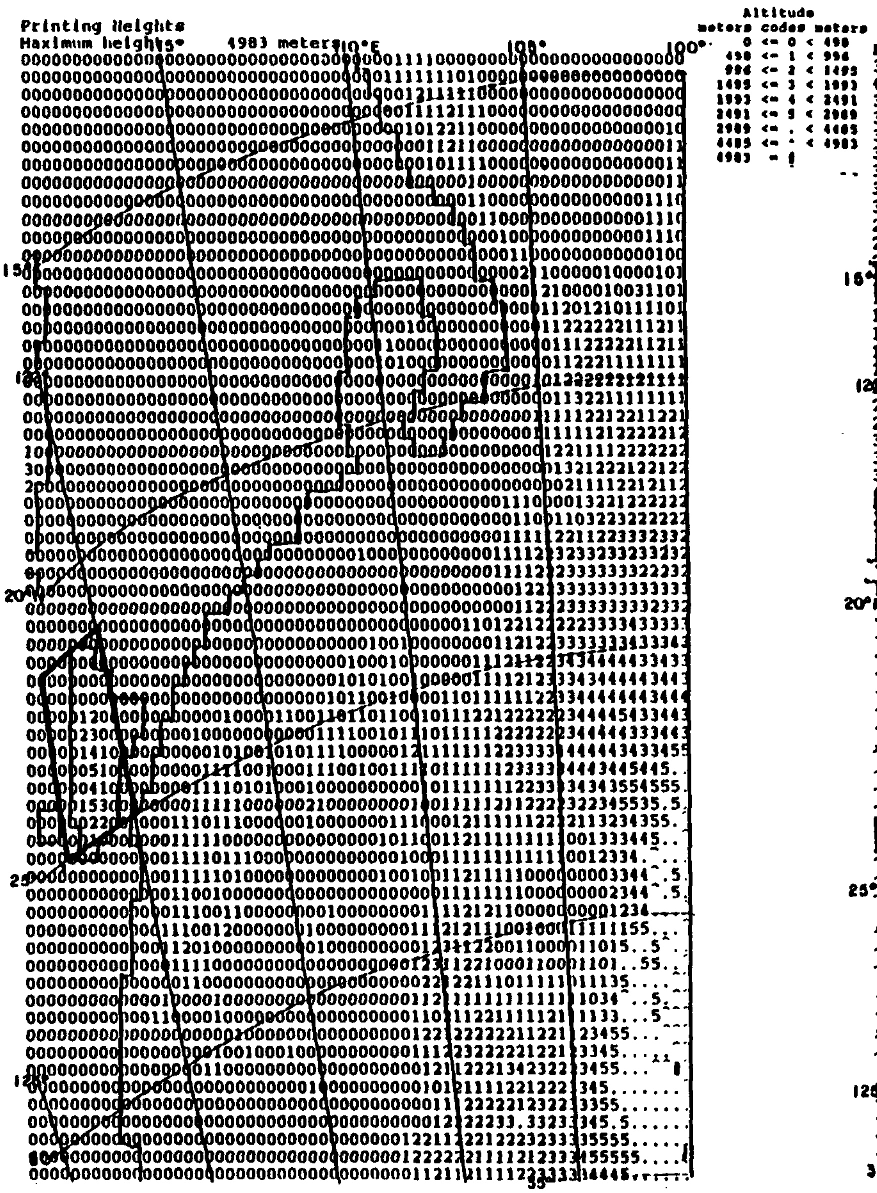

Figure 15c. Altitudes.

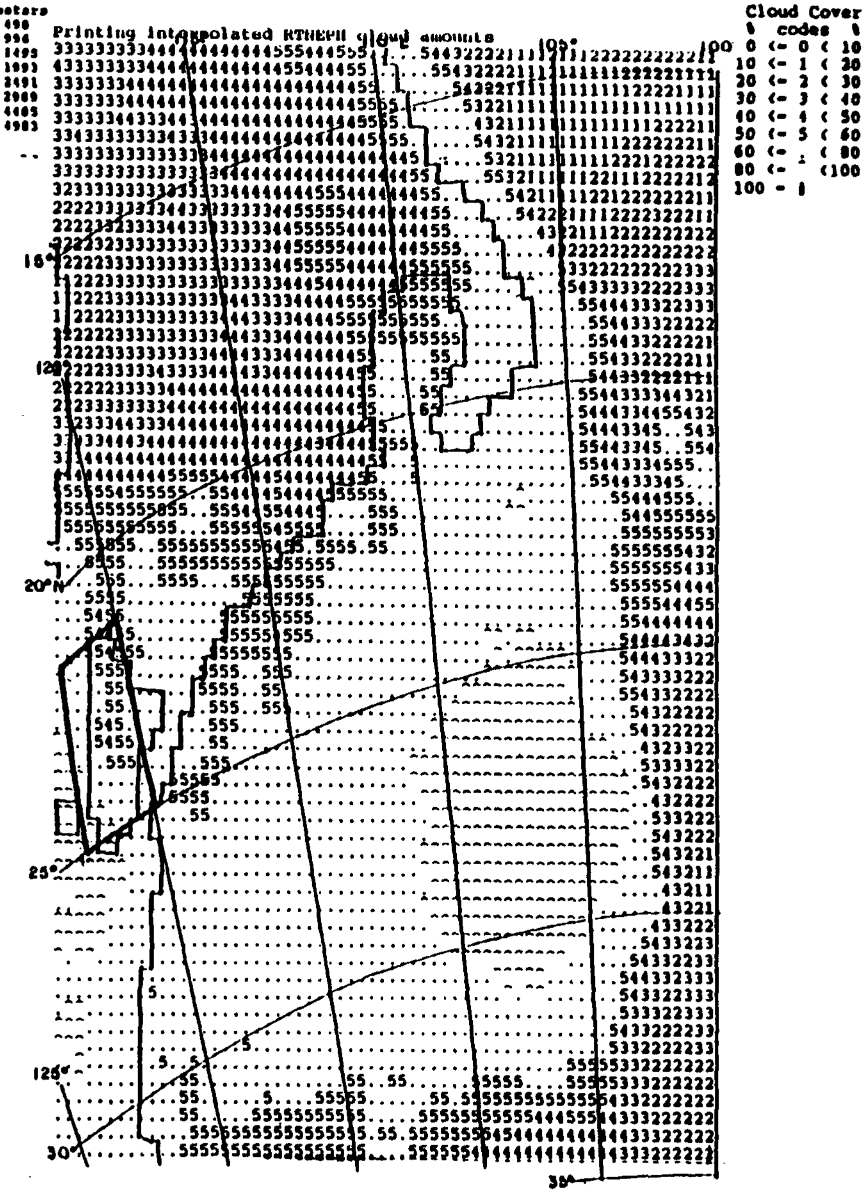

Figure 15d. RTNEPH Amounts.

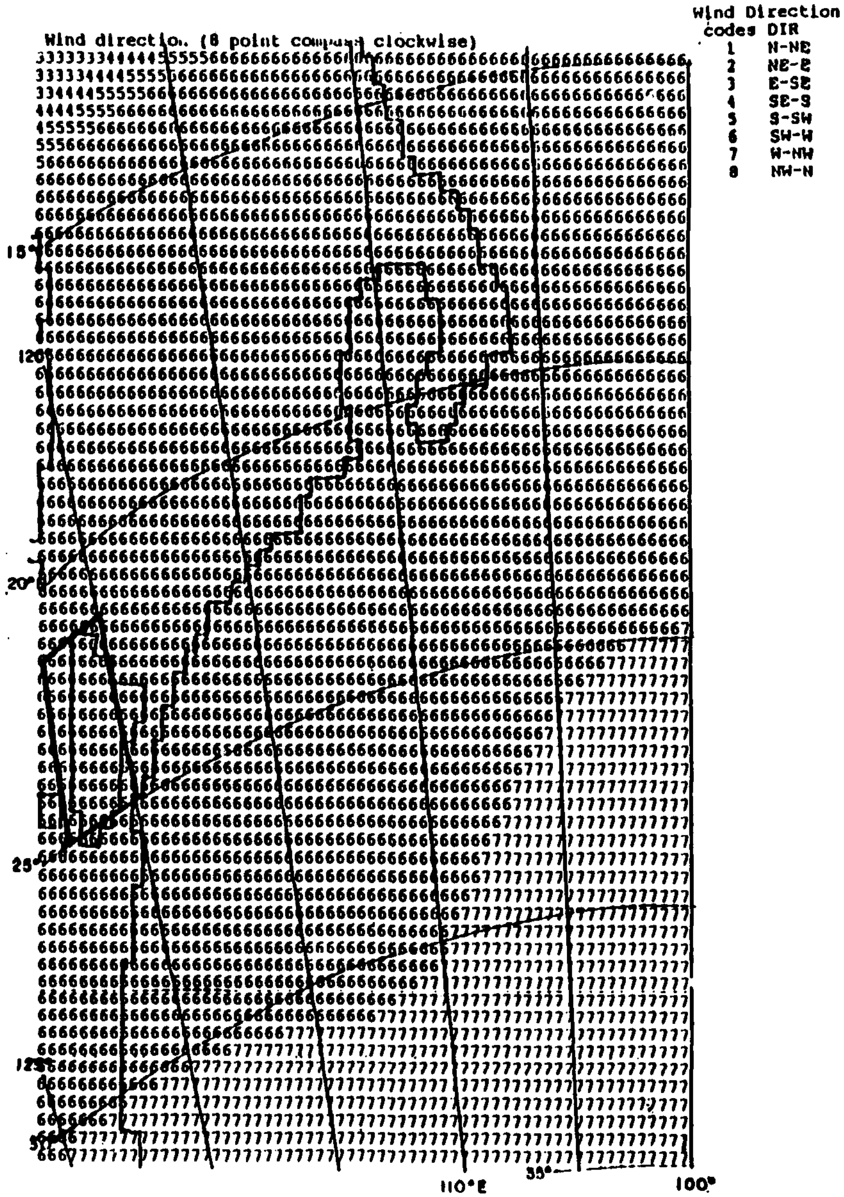

Figure 15e. Vector Mean Wind Directions.

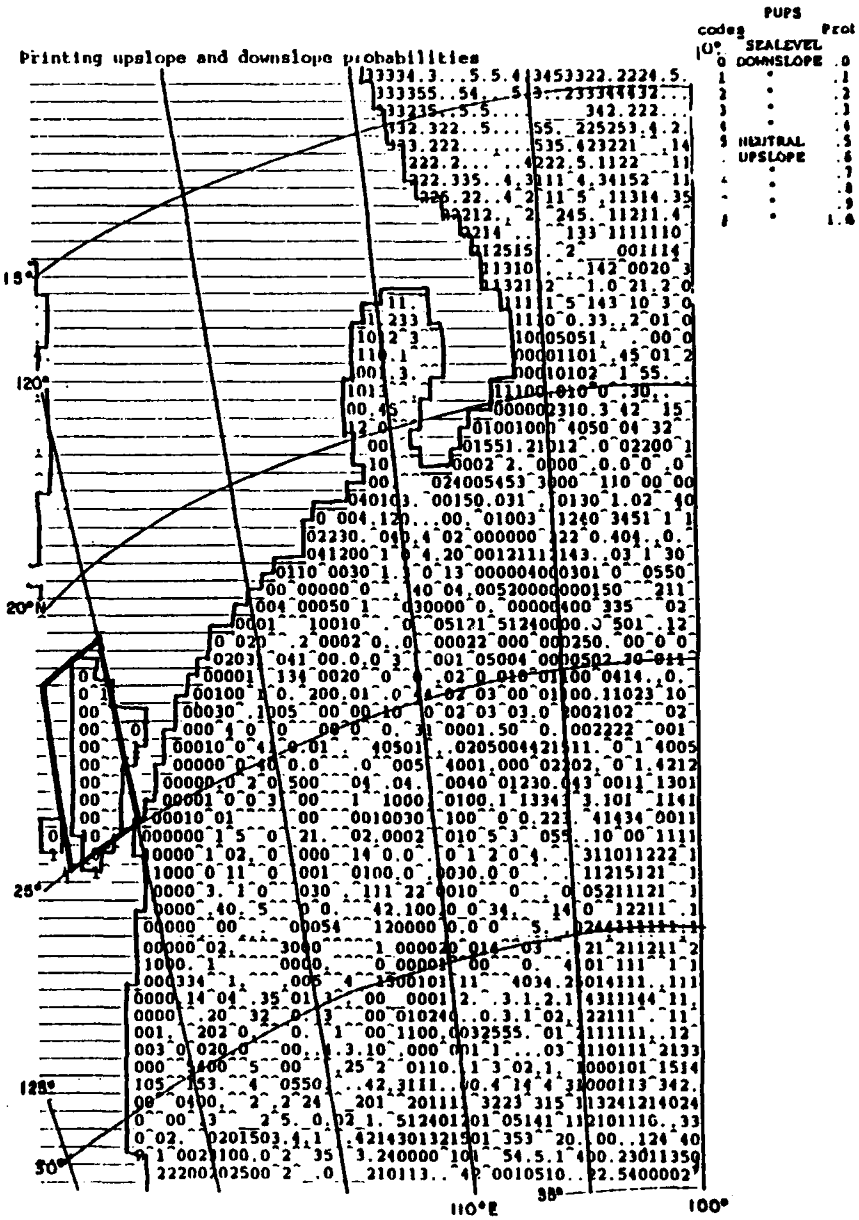

Figure 15f. Upslope Probabilities.

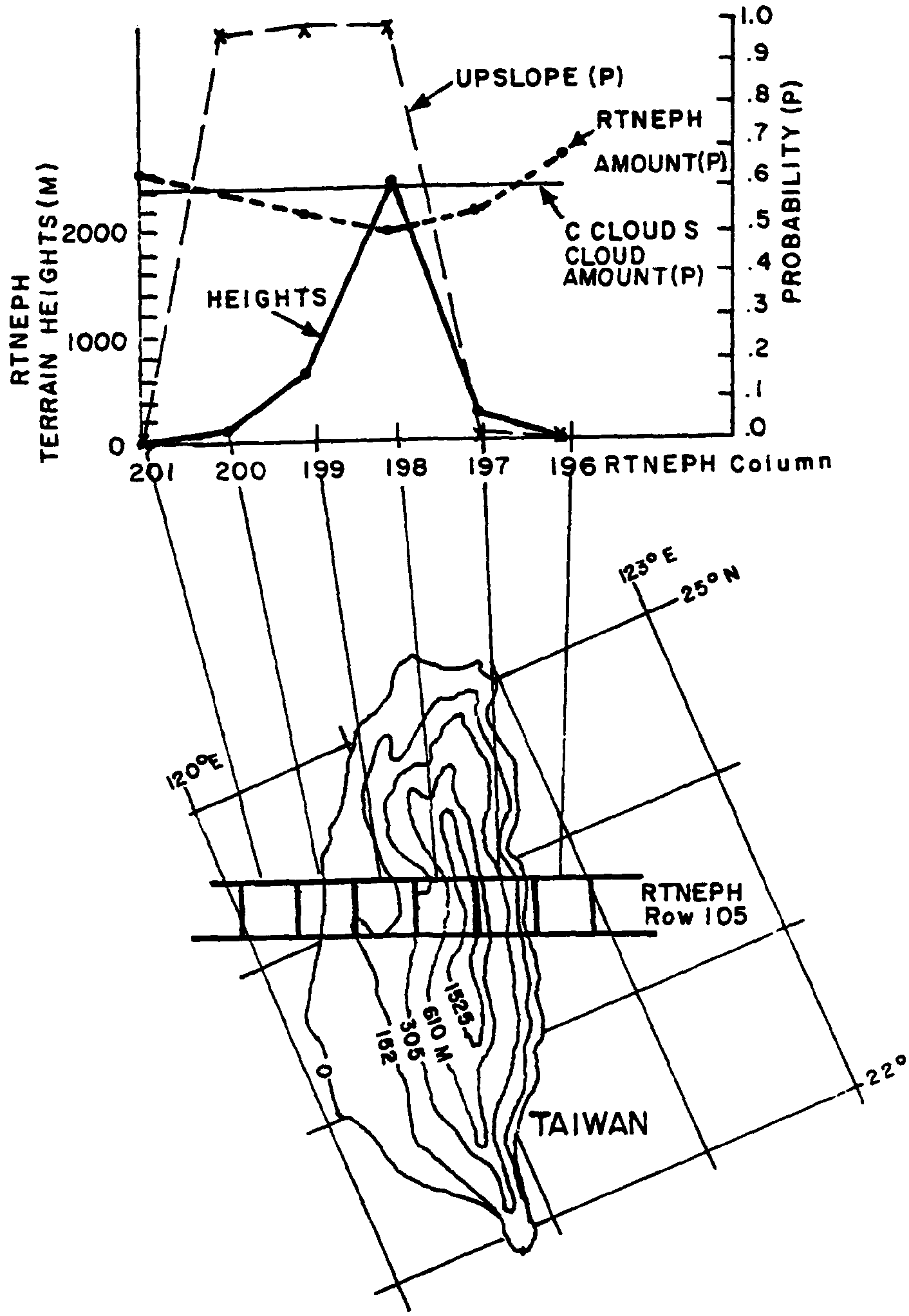

Figure 16. Four Parameters are Portrayed (Top) that are Associated with the Foot Prints (Map Columns) Detailed Along the NH Map Row #105 that Crosses Over Central TAIWAN (Bottom). The Values Portrayed are Typical at all Row and Column Positions Over the Island. Note that the Mean RTNEPH Amount is Lower Over the Highest Terrain Points and Higher Over the Lower and Surrounding Ocean Areas Despite the Large Increase of Upslope Probability Over the Windward Side of the Island.

conditions over hilly terrain areas was generally not supported in this investigation does not mean that upslope flow never causes small cloud development. Perhaps it doesn't occur often enough to show up in the long term climatology and/or the 25 nautical mile resolution of the RTNEPH data is not fine enough to pick up the smaller scale mountain effects. Of the cases studied, blockage of clouds by hilly terrain appears to be a major cause of the observation of large amounts of mean cloudiness along mountain chains.

Comparisons between cloud amount climatologies from the RTNEPH with those indicated using C Cloud S reveals that a much finer resolution cloud database is required to produce predictors capable of indicating accurate cloud amounts within valleys and over mountainous terrain.

The detailed case studies in this report do show that improved mathematical indicators are needed in order to indicate small scale mean cloud amount conditions over certain areas of the world.

REFERENCES

Hoke, J. E.,et al, 1981: Map Projections and Grid Systems for Meteorological Applications. United States Air Force, Air Weather Service (MAC), Air Force Global Weather Central, Offutt AFB, NE.

Burger, C. F.,1985: World Atlas of Total Sky Cover. AFGL-TR-85-0198. Air Force Geophysics Laboratory, Hanscom Air Force Base, MA. ADA-170474.

Hahn, C. J.,1987: Climatological Data for Clouds Over the Globe from Surface Observations. Cooperative Institute for Research in Environmental Sciences, University of Colorado, Boulder, CO.

Hwang, P. H., L.L. Stowe, H.Y. Michael Yeh, H. Lee Kyle, And the NIMBUS-7 Cloud Data Processing Team, 1988b: The NIMBUS-7 Global Cloud Climatology. Bull Amer. Meteor. Soc., 69 743-752.

Barker-Schaaf, C., et al, 1990: The Hemispheric Eighth Mesh Terrain Elevation and Geography Data Sets. GL-TR-90-0223, Special Reports, No. 263 (ASD), Geophysics Laboratory, Hanscom AFB, MA 01731-5000, ADA-231592.

Dalcher, A., 1992: Cloud-Free Line-of-Sight (CFLOS) Availability. Institute for Defence Analysis, IDA paper p-2655.

Willand, J. H., 1992: Database Blending for the Climatology of Cloud Statistics Program. PL-TR-92-2344, Final Report. Phillips Laboratory, Directorate of Geophysics, Air Force Materiel Command, Hanscom Air Force Base, MA. ADA265034.

Boehm, A., J. Willand, and G. Gray, 1993: Reconciling Satellite and Surface Cloud Observations. Reprints - Eighth Applied Climatology Conference, Jan 17-22, 1993, Anaheim, CA. Published

by the American Meteorological Society, Boston, MA.

Boehm, A., J. H. Willand, 1993: C CLOUD S "See Clouds" Climatology of Cloud Statistics, Version 0.94. Computer Program Developed for the United States Air Force Phillips Laboratory, Geophysics Directorate. Hanscom Air Force Base, MA.